Article

Modified Natural Clinoptilolite Alleviates Cadmium-Induced Toxicity in Icr Albino Mice

Michaela Beltcheva *, Yana Tzvetanova, Peter Ostoich, Iliana Aleksieva, Tsenka Chassovnikarova *, Liliya Tsvetanova, Rusi Rusew

Posted Date: 26 March 2025

doi: 10.20944/preprints202503.1874.v1

Keywords: clinoptilolite; mice; cadmium toxicity; clinoptilolite detoxification; hematological parameters; oxidative stress; micronuclei frequency

Article

Modified Natural Clinoptilolite Alleviates Cadmium-induced Toxicity in ICR Albino Mice

Michaela Beltcheva [1], Yana Tzvetanova [2], Peter Ostoich [1], Iliana Aleksieva [1], Tsenka Chassovnikarova [1,3,*], Liliya Tsvetanova [2] and Rusi Rusew [2]

[1] Institute of Biodiversity and Ecosystem Research, Bulgarian Academy of Sciences, 1 Tsar Osvoboditel Blvd., 1000 Sofia, Bulgaria

[2] Institute of Mineralogy and Crystallography Acad. I. Kostov, Bulgarian Academy of Sciences, Acad. G. Bonchev Str., bl. 107, Sofia 1113, Bulgaria

[3] Plovdiv University, Faculty of Biology, Department of Zoology, 4 Tzar Assen Str., Plovdiv 4000, Bulgaria

* Correspondence: t.tchasovnikarova@gmail.com

Abstract: For the first time, this study investigates *in vivo* the potential of Na-modified natural clinoptilolite to mitigate cadmium toxicity in ICR mice, a model relevant to human health. We enhanced natural clinoptilolite to improve its Cd^{2+} exchange capacity. Mice were exposed to environmentally realistic Cd(NO3)2 doses in their drinking water. The detoxification efficacy of the mineral was evaluated over 45 days in four groups: control (no supplementation), $Cd(NO_3)_2$ only, clinoptilolite only, and a combination of $Cd(NO_3)_2$ and clinoptilolite. We assessed Cd bioaccumulation in the liver and kidneys, genotoxicity (micronucleus assay), hematological parameters, and oxidative stress markers. Cd exposure resulted in significant bioaccumulation, reduced growth, changes in the erythrogram, DNA damage, and oxidative stress. Mice receiving clinoptilolite alone showed a significant increase in body mass. Modified clinoptilolite led to nearly a 48% reduction in Cd accumulation and a 30% increase in Cd-excretion in the Cd-plus-clinoptilolite group compared to the Cd-only group. Erythrogram and leukogram parameters returned to near-normal levels, with reductions in malondialdehyde (MDA) and increases in glutathione (GSH) observed by the end of the experiment. No elevated levels of micronuclei were found following zeolite supplementation. These results suggest modified clinoptilolite may be a cost-effective detoxifier in Cd-polluted regions.

Keywords: clinoptilolite; mice; cadmium toxicity; clinoptilolite detoxification; hematological parameters; oxidative stress; micronuclei frequency

1. Introduction

Heavy metals have numerous sources of exposure, routes, and distinct biotransformation and elimination pathways [1]. In recent years, natural zeolites have gained popularity as an effective solution for metal removal due to their advantageous properties and structural characteristics. Consequently, they are utilized across various industrial, agricultural, environmental, and biological applications [2,3].

The minerals of the clinoptilolite series (clinoptilolite-Ca, clinoptilolite-K, clinoptilolite-Na) are the most abundant natural zeolites with HEU-type framework topology and Si/Al ratio greater than 4 [4]. They have monoclinic symmetry, space group C2/m, which may be lowered to C2 or Cm [4,5]. The HEU-type topology is characterized by a two-dimensional system of three types of channels, which is defined by ten- and eight-membered tetrahedral rings. The large ten-membered A channel and the smaller eight-membered B channel are parallel to the *c*-axis, and both intersect the eight-membered C channel, which is parallel to an *a*-axis [6–9]. The channels are occupied by extra-framework cations (Na^+, K^+, Ca^{2+}, Mg^{2+}, Ba^{2+}, and Sr^{2+}), which are coordinated by H_2O molecules in irregular polyhedral and/or framework oxygens [10]. Four extra-framework cation positions are

 doi:10.20944/preprints202503.1874.v1

recognized in the tetrahedral framework of the HEU-type zeolite: M(1), M(2), M(3), and M(4) [8]. The wide variability of the cation exchange properties of clinoptilolite depends on the Si/Al ratio, the specific position of the extra-framework cations within the structure, their coordination by H_2O molecules, and interactions with framework oxygens [10,11].

In Bulgaria, sizable deposits of high-quality zeolites, mainly clinoptilolite, are present in the eastern parts of Rhodopes Mountain. Five clinoptilolite and one mordenite deposits were identified and explored by drilling. They are related to the Paleogene volcanism's first and second Rupelian acid volcanic phases [12–15].

Natural zeolites possess unique qualities that may render them an attractive alternative to currently available chelating agents for removing heavy metals from blood, tissues, and adipose stores [16]. Natural clinoptilolite is not a chelator in the traditional sense; instead, it operates through ion exchange and adsorption. Due to its low cost, natural clinoptilolite has been the focus of numerous *in vitro* studies exploring its sorption properties and interactions with biological systems at the cellular and molecular levels. In contrast, *in vivo* studies examining the heavy metal sorption capacity of natural clinoptilolite in biological models (specifically laboratory mice) are scarce and mainly focused on the removal of lead (Pb) [17–19]. The results indicate that 30% to 70% of the ingested Pb is adsorbed by zeolite in the gastrointestinal tract and subsequently excreted from the body in the feces [17–19]. [20] suggests that clinoptilolite does not impact the organism's homeostasis of trace elements but shows notable selectivity for heavy metals and toxic substances. There are assumptions and indirect evidence that the mineral influences the redox status of the organism based on its well-defined ion exchange potential [20–22].

The primary parameters used to assess organisms' health status and provide an early warning of potentially harmful physiological changes due to xenobiotic exposure include heavy metal bioaccumulation, hematological indices, oxidative stress, and DNA damage assessments. The pattern of Cd bioaccumulation results in toxicity, which can potentially cause adverse effects on organisms, including growth inhibition [23], oxidative and mitochondrial stress, and apoptosis [24,25]. Cd is known to have a long half-life [26]. Following absorption, Cd accumulates primarily in the liver and kidneys, presenting a significant risk of severe hepatotoxicity and nephrotoxicity [27,28]. The liver is a major target organ during acute Cd exposure, while the kidneys are significantly affected by prolonged exposure to Cd [29]. The enterohepatic circulation of Cd induces the synthesis of metallothionein (MT) and the formation of Cd-MT complexes, preventing Cd from reacting with target molecules [30]. This makes Cd less accessible for sorption, and the effectiveness of clinoptilolite may depend on its ability to release Cd from these complexes.

A comprehensive investigation into the impact of heavy metals on organisms indicates that blood may serve as an effective biomarker for Cd exposure and toxicity *in vivo* [1] due to its accessibility and the range of measurable parameters, which makes it a powerful tool. Hematological parameters are frequently used in mammalian medicine. Cd has been demonstrated to cause significant alterations in the blood biomarkers in mice [31–33], including a reduction in hemoglobin (Hb), hematocrit (Hct), and red blood cell (RBC) count, along with increases in white blood cell (WBC) count [34–36]. Only a few studies have reported changes in hematological indices, such as leukocyte and thrombocyte counts, during hemoperfusion with clinoptilolite [18,20].

Oxidative stress caused by the generation of reactive oxygen species (ROS), including superoxide ions, hydrogen peroxide, and hydroxyl radicals, is considered a significant mechanism underlying Cd-induced toxicity [37]. This process compromises antioxidant defense mechanisms and increases ROS production by mitochondria as by-products of oxidase activities [38]. Furthermore, studies show that Cd impacts glutathione (GSH) levels, a tripeptide that plays a crucial role in non-enzymatic antioxidant protection. Research indicates that Cd initially depletes GSH stores by inhibiting GSH synthesis and enhancing GSH oxidation [37]. This process acts as the first line of defense against Cd-induced toxicity [39]. Clinoptilolite has shown promise in *in vitro* studies for reducing oxidative stress, primarily through its ability to eliminate heavy metals and its potential to influence antioxidant enzyme activity [21,22].

 doi:10.20944/preprints202503.1874.v1

The formation of micronuclei (MNs) has been extensively utilized as a biomarker of genotoxic stress and genetic instability in many human and non-human models [40]. It has been demonstrated that MN formation is elevated in the peripheral blood erythrocytes of mice residing in areas contaminated with Cd [41,42]. The prolonged exposure to elevated concentrations of Cd exerts genotoxic effects on peripheral blood and bone marrow cells in rats, such as DNA damage, leading to mutations and chromosomal aberrations and the formation of MNs [43–45]. Their mechanisms include inhibiting DNA repair and direct reactivity with DNA phosphate groups [46]. Direct research assessing the influence of clinoptilolite on micronuclei (MNs) formation is lacking; however, some studies touch upon the genoprotective potential of clinoptilolite, which is relevant to MN formation [47].

The slow elimination rates and biomagnification of Cd in higher levels of food chains in ecosystems [47,48] are expected to create serious problems in the next decade [49]. Consequently, the ongoing challenge of removing accumulated Cd remains a significant concern [50]. The long-term effects of clinoptilolite on biological systems, including its potential toxicity and biocompatibility, must be thoroughly investigated. In this regard, conducting an *in vivo* study incorporating appropriately activated natural clinoptilolite as a Cd^{2+} sorbent in ecotoxicological experiments with model mammal organisms warrants further exploration. The potential of modified natural clinoptilolite to detoxify Cd in mammalian organisms must be thoroughly evaluated through oral administration due to the harsh conditions of the gastrointestinal tract, including varying pH levels and digestive enzymes. Clinoptilolite's ability to reduce heavy metal absorption in the gastrointestinal tract is crucial for human health, and studies that focus on oral administration may be more relevant for human applications. Accordingly, this study aimed to enhance the Cd^{2+} exchange capacity of natural zeolite clinoptilolite from the "Beli Plast" deposit through Na-activation and to evaluate its protective efficacy as a Cd-sorbent to reduce hepatic and renal Cd bioaccumulation, Cd-induced oxidative stress, hematological alterations, and genotoxic damage in ICR mice. The formulation of the resulting modified clinoptilolite is of the utmost importance, as it must incorporate elements deemed safe for utilization in mammalian models.

This study proposes that Na-activated modified zeolite clinoptilolite can absorb significant amounts of Cd2+ ions in the digestive tract, thereby reducing levels of Cd intoxication, as indicated by changes in physiological and genetic parameters. The study hypothesizes that Cd bioaccumulation, hematological indices, oxidative stress, and DNA damage will differ before and after clinoptilolite supplementation. The mineral is expected to mitigate the severity of Cd-induced physiological changes and DNA damage.

2. Materials and Methods

2.1. Clinoptilolite

The clinoptilolite-rich tuff used in this study was collected from the volcanogenic sedimentary deposit Beli Plast, located in the Eastern Rhodopes region of Bulgaria (Figure 1). This deposit is related to the first Rupelian acid volcanic phase that occurred at the beginning of the Oligocene. In the shallow marine environment, the metastable volcanic glass transformed into more stable phases predominantly composed of clinoptilolite [12–14].

 doi:10.20944/preprints202503.1874.v1

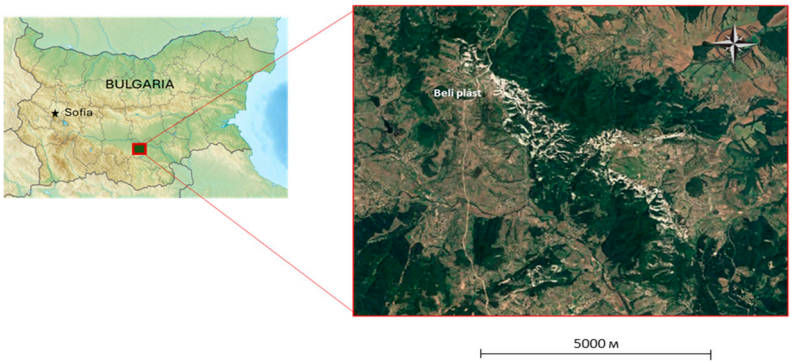

Figure 1. Clinoptilolite deposits in the Eastern Rhodopes area near Beli Plast village.

2.1.1. Samples Collection

Samples of clinoptilolite-rich tuffs from the four major Bulgarian deposits—Beli Plast, Golobradovo, Most, and Beliya Bair—were collected to identify a suitable material for clinoptilolite sorbent. Their mineral and chemical compositions were analyzed to select a material for use in eco-toxicological experiments as a sorbent combined with traditional food (Table S1, Figure 2).

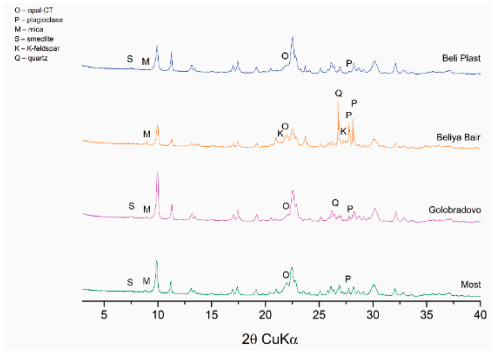

Figure 2. Powder X-ray diffraction patterns of the studied clinoptilolite-rich tuffs. The minerals in association with clinoptilolite are depicted.

European legislation has allowed a limited concentration of toxic metals in clinoptilolite tuffs used as food additives [51]. The EU Regulation [52] permits using sedimentary clinoptilolite as a food additive. It authorizes the use of zeolitized tuff if the clinoptilolite content is ≥ 80%, clay minerals are ≤ 20%, and it is free of fibers and quartz. According to these regulations, the clinoptilolite-rich tuffs from the Beli Plast deposit are particularly suitable for use as a mineral additive since the levels of Pb and Cd are below the maximum permissible values of 60 ppm and 5 ppm, respectively. The concentration of As is under the detection limits (Table S1). The tuffs contain > 80% clinoptilolite and < 20% montmorillonite and are free of quartz (Figure 2).

2.1.2. Preparation of Na-Exchanged Clinoptilolite Sorbent

The ion-exchange method is regarded as relatively cost-effective and efficient for removing hazardous metals. According to [53], Na-exchanged clinoptilolite has a greater Cd exchange capacity than the natural form. To prepare a sorbent for detoxification, clinoptilolite tuff from the Beli Plast deposit was ground and sieved, with the fraction below 0.15 mm being separated for treatment. The Na-exchanged sample was prepared by stirring 100 g of the natural sample with 1000 ml of a 1 M $NaNO_3$ solution at 500 rpm. The experiment was performed at 80 °C in a closed bottle. The $NaNO_3$ solution was replaced daily with a fresh one. This procedure was repeated 12 times, after which the sample was washed with deionized water and dried at 60 °C.

 doi:10.20944/preprints202503.1874.v1

After Na-exchange, the sample is mechanically tribe-activated using the ball-mill method to enhance the selective properties of clinoptilolite by reducing particle size and increasing the surface area of the zeolite material.

2.1.3. Characterization Methods

Powder X-ray diffraction (PXRD) analysis was conducted using a PANanalytical EMPYREAN diffractometer with a goniometer radius of 240 mm. The system operated at 40 kV and 30 mA, utilizing CuKα radiation, and included a 3D pixel detector. PXRD measurements were taken at room temperature across the 2θ range of 3–70° with a scanning rate of 0.013° over 80 seconds.

The chemical composition of the major elements was determined using inductively coupled plasma optical emission spectrometry (ICP-OES). Trace element contents were obtained through laser ablation inductively coupled plasma mass spectrometry (LA-ICP-MS) with a PerkinElmer ELAN DRC-e ICP-MS and a New Wave UP193-FX excimer laser system. The element concentrations represent average values derived from three measurements of pellets prepared with lithium tetraborate at 1050 °C.

Scanning electron microscopy (SEM) and electron probe microanalysis (EPMA) were utilized to analyze individual clinoptilolite grains' morphology and chemical compositions. This was conducted using a ZEISS EVO 25LS scanning electron microscope (Carl Zeiss SMT Ltd, Cambridge, England) equipped with an EDAX Trident system, operating at a 16 kV accelerating voltage and approximately 1 nA beam current, with reference standards.

The particle size distribution of the clinoptilolite powder was performed using laser diffraction and the wet dispersion method. Tests were conducted using a Mastersizer 3000 Malvern-Panalytical device.

Dynamic Light Scattering (DLS). The size of particles smaller than 6 μm in Na-exchanged and tribo-activated clinoptilolite was obtained using the Dynamic Light Scattering (DLS) technique. The particle size distribution was determined at 657 nm and 90 degrees using Dynamic Laser Scattering measured by a goniometer from Brookhaven Instruments Corporation Bi-90 plus, equipped with a correlator and avalanche photodetector (APD), New York, USA. The particle size measurement ranges from 1 nm to 6 μm and conforms to ISO 2241 and ISO 13321 standards. The measurement conditions for tribo-activated particles of clinoptilolite in diluted aqueous solution were conducted at 25 °C, with an average count rate of 396.03 kcps in 3 ml disposable polystyrene cuvettes. The measurements were performed in triplicate (one run consists of three cycles of 3 minutes). Data were analyzed using the Particle Solutions (version 3.6.0.7136) software.

The textural parameters of the clinoptilolite powder, including the specific surface area and pore volume, were measured using nitrogen adsorption/desorption at −196 °C with the Micromeritics 3Flex surface characterization analyzer. Before the test, the samples were outgassed at 200 °C to attain a constant mass. The specific surface area was calculated using the Brunauer–Emmett–Teller (BET) method.

2.2. Experimental Design

The present study was a one-way, four-variant experiment that was conducted using ICR (CD-1) mice. The four experimental variants were as follows: control group (C): mice had ad libitum access to a nutritionally complete solid conventional rodent food free of Cd; zeolite group (Z): the mice were administered a standard rodent food supplemented with 12.5 wt.% powdered modified natural zeolite-clinoptilolite; Cd group (CDw): the mice received an oral solution of 0.00125M $Cd(NO_3)_2$, dissolved in deionized water and administered through their drinking water while maintaining a standard rodent diet; Cd + Zeolite group (CDwZ): the mice were orally administered a 0.00125M $Cd(NO_3)_2$ solution and provided with standard rodent food containing 12.5 wt.% powdered modified natural clinoptilolite. The $Cd(NO_3)_2$ concentration is considered an intermediate dose that is environmentally realistic, supported by previous studies that simulate the exposure of mammals and humans in industrially polluted areas to Cd contamination through food or water [54,55].

 doi:10.20944/preprints202503.1874.v1

The four experimental variants were conducted over 45 days, during which the body mass of the animals and the necessary blood samples were collected from each experimental group at the same sampling times for each variant on the 0th, 15th, 30th, and 45th days. The obtained animal body mass was then compared to the established norms for the ICR strain of laboratory mice of the same age and sex. [56]. The total sample size was calculated before the experiment, estimating an effect size of 0.4, a probability level (α) of 0.05, and a power (1-β) of 0.95. Eight mice were chosen to satisfy statistical requirements for a small group at each time point. Each group had a total of 32 mice, leading to an overall sample size of 128. Mice were randomly assigned to treatment groups via a random number generator, using block randomization with a block size of 8 for equal group sizes. The treatment order within each block was determined using Excel's RAND function. Blinding was performed during the experiment concerning the allocation group, along with the outcome assessment and data analysis.

2.3. Experimental Animals and Husbandry

Only healthy ICR (CD-1) mice bred in the certified vivarium at the Institute of Neurobiology, Bulgarian Academy of Science, with health records and no signs of illness or injury, were included in the study. Male mice aged 6 to 8 weeks weighing 25 to 30 grams were used to ensure group homogeneity. The mice were housed in individual, well-ventilated and randomly assigned to shelf positions cages in the Institute of Biodiversity and Ecosystem Research vivarium following European standards (Directive 2010/63/EU). The bedding material was sourced from an ISO 2000-accredited supplier. Before the experiments began, the mice were acclimatized for seven days. The study was maintained within a controlled environment at a standard temperature between 20°C and 22°C, a 45-60% humidity range, and a 12-hour light/dark cycle. The mice were given standard pelleted rodent food and had access to food and water *ad libitum*. The water, food, and bedding materials were checked daily, and replacements were made as needed. The animals were neither given medication nor vaccinated. Animals showing severe distress (e.g., persistent vocalization, self-mutilation), losing over 20% body weight, illness, or abnormal behavior affecting data were excluded due to potential impact on physiological parameters studied. All the experiments were conducted following Ordinance No. 20/01.11.2013 on the protection and welfare of animals and the Animal Protection Act of 31 January 2008 of the Republic of Bulgaria and approved by the Institute of Biodiversity and Ecosystem Research Ethical Committee.

2.4. Heavy Metal Loading

Cd concentration was determined using a Perkin Elmer SCIEX DRC-e ICP-MS system equipped with a cross-flow nebulizer. The spectrometer (RF, gas flow, lens voltage) was optimized to yield minimal CeO^+/Ce^+ and Ba^{2+}/Ba^+ ratios, while maximizing the intensity of the analytes. Working standard solutions of Cd, within a concentration range of 0.01 to 500 μg L^{-1}, were prepared from a single-element calibration solution (Merck) with an initial concentration of 1000 mg L^{-1}. External calibration was conducted for isotopes $^{111, 112, 113, \text{and } 114}$ Cd. The calibration coefficients for all calibration curves were at least 0.99. The evaluation was performed by analyzing two certified reference materials: IAEA-H-8 horse kidney and NIES N6 CRM mussel. The calibration and sample analysis results were consistent with the certified values.

2.5. Weight and Organ Index Assays

Throughout the treatment period, the body weight of each mouse was measured at every experimental time point, and any changes were documented. The liver and kidneys were weighed accurately to determine the organ indices, which were calculated as follows: organ index (%) = average weight of the organ / (average body weight) × 100%.

 doi:10.20944/preprints202503.1874.v1

2.6. Hematology

Blood samples were collected from the tail vein into 0.5 mL MicroTube EDTA K3 microtubes and were automatically analyzed using a MindRay BC-30Vet automated veterinary hematology analyzer. The following parameters were chosen as the most representative for research purposes: red blood cell (RBC) and white blood cell (WBC) counts, hemoglobin (Hb), hematocrit (Hct), mean corpuscular volume (MCV) of the RBC, and mean corpuscular hemoglobin (MCH) in RBC.

2.7. Oxidative Stress Markers

Two markers for oxidative stress were selected for analysis: 1) the presence of malondialdehyde (MDA) in organ homogenates, measured by the thiobarbituric acid-reactive substances (TBARS) test, serving as a biomarker for lipid peroxidation, and 2) the total amount of glutathione (GSH) in the same organ homogenates. The TBARS test was conducted as described in [57]. Mouse liver and kidneys were homogenized and subjected to the procedure described. MDA levels were measured spectrophotometrically by absorbance at 532 and 600 nm and expressed as nmol MDA/g of fresh weight. Total glutathione was assessed calorimetrically, following the protocol outlined by [58]. Glutathione levels were presented as mmol GSH/g of tissue.

2.8. Micronucleus Test

To evaluate the potential for genotoxic effects caused by exposure to environmentally relevant $Cd(NO_3)_2$ concentrations, an in vivo micronucleus test was conducted using a slightly modified version of the original acridine orange staining technique [59]. Instead of phosphate-buffered saline (PBS), Sörensen's sodium phosphate buffer (pH 7.4) was used. Image acquisition and analysis took place on an OPTIKA B-383 FL fluorescence microscope at a magnification of 400x, employing a blue filter set (excitation wavelength 460–490 nm, emission at 515 nm). Micronuclei (MNs) were categorized as such when they showed a similar yellowish-green staining pattern and focusing configuration as the main nucleus, exhibited a round or oval shape, and did not exceed one-third of the main nucleus's size. The mean frequency of recorded micronuclei refers to the number of cells with MNs per 2,000 counted erythrocytes, expressed per thousand (‰).

2.9. Statistical Analysis

A power F test analysis for one-way ANOVA fixed effects was performed before the experiment commenced using the G*Power software program to compute the estimated effect and sample size. The statistical significance of the mean differences between the tested parameters was calculated using Prism software, version 9.0 (GraphPad Software, San Diego, CA, USA). Both univariate and multivariate statistical analyses were conducted. The variability of the parameters under examination was evaluated through univariate statistical analysis. The results are presented as mean ± standard deviation. To ascertain the normality of the data and the homogeneity of variance, the D'Agostino-Pearson and Levene F-tests were employed. The normality of the hematological data was assessed ($p < 0.001$), and a one-way ANOVA was conducted, followed by Tukey's multiple comparison post-test. A nonparametric analysis was necessary because the data on MNs did not meet the normality test requirements. As a result, the Kruskal-Wallis nonparametric multiple comparison test with Dunn's post hoc test was utilized. The significance level was set at $p \leq 0.05$.

3. Results

3.1. Characterization of the Natural and Na-Exchanged Clinoptilolite Tuff

The mineral composition of the clinoptilolite-rich tuff from the Beli Plast deposit was determined using PXRD. The mineral quantities obtained from the sample studied are as follows (in wt. %): clinoptilolite ~86%, opal-CT ~7%, mica(10Å) ~2%, montmorillonite ~2%, and plagioclase ~2% (Figure 2).

 doi:10.20944/preprints202503.1874.v1

Table 1 presents the chemical composition of the major elements (in wt.%) for both natural and Na-exchange samples. The Na_2O content significantly increases after sodium exchange, reaching 4.26 wt.%, while the values for the oxides of the exchangeable cations (CaO, K_2O, and MgO) decrease.

Table 1. Chemical composition of the natural clinoptilolite-rich tuff and Na-exchanged sample from Beli Plast deposit.

	SiO_2	TiO_2	Al_2O_3	Fe_2O_3(t)	MnO	MgO	CaO	Na_2O	K_2O	SO_3	LOI	H2O–	Total
Natural clinoptilolite tuff	71.08	0.12	10.88	0.96	0.09	1.03	2.78	0.31	2.76	0.15	9.3	2.31	101.77
Na-exchanged sample	69.42	0.14	10.63	0.82	0.08	0.58	0.9	4.26	2.46	0	9.13	3.56	101.98

The content of 63 trace elements was measured to screen for toxic and potentially toxic elements in the clinoptilolite tuff. The element concentrations were converted into true values through internal standardization (concentration of Si, determined by ICP-OES). The concentrations of the trace elements were compared to average concentrations for the upper continental crust [60]. The contents of the elements As, Cd, Co, Ge, Se, Mo, Te, Eu, Pd, Re, Rh, and Au are below the detection limits (Table S1). The LA-ICP-MS data reveal that the clinoptilolite tuff is relatively depleted in Sc, V, Cr, Ni, Cu, Zn, Ga, Y, Zr, Ba, Hf, W, and REE (except for lanthanum, thulium and ytterbium). Relative enrichment is found for Cs, Ta, Tl, Pb, Bi, Th, U, Be, S, Rb, Sr, Nb, In, Sn, Sb, and Ag [61]. Regarding the contents of the toxic elements, the clinoptilolite-rich tuff from the Beli Plast deposit is suitable for usage as a sorbent for detoxification purposes because the contents of Pb and Cd are lower than the maximum permissible values and the concentration of As is below the limits of detection (Table S1).

The morphological characteristics of the clinoptilolite-rich tuff from the Beli Plast deposit are shown in Figure 3. Typically, clinoptilolite forms fine crystals (<5 μm) and pseudomorphically replaces both pumice and shards (Figure 3a). It rarely occurs as prismatic crystals up to 30 μm long in the central hollows of the glass shards (Figure 3b–d).

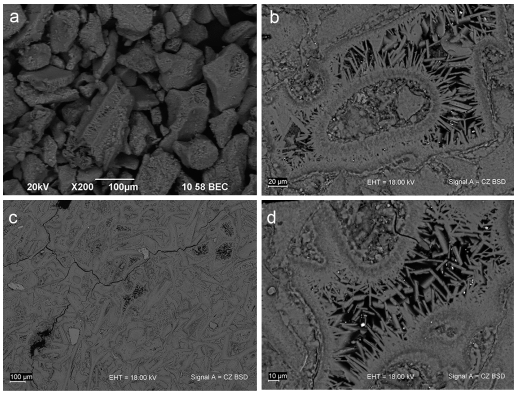

Figure 3. Back-scattered electron images (BSE) images of the used fraction < 0,15 mm (a); poorly crystalline clinoptilolite (c) and prismatic crystals up to 30 μm long (c-d) (b–d –polished sections).

Electron probe microanalyses show slight variations in the chemical composition of the studied clinoptilolite grains (Table 2). The crystal-chemical formulas are calculated based on 72 oxygens. The Si/Al ratios determined by EPMA range from 4.22 to 4.71.

 doi:10.20944/preprints202503.1874.v1

Table 2. Chemical composition (EPMA, wt%) and crystal-chemical formulas of the separate clinoptilolite grains from Beli Plast deposit (based on 72 oxygen atoms).

Samples Oxides	P1-17	P1-19	P1-12	P1-13	P1-14	P1-15	P1-16
SiO2	69.07	70.74	66.90	68.19	66.97	67.88	68.46
Al2O3	12.70	12.82	13.44	13.38	13.38	12.31	12.34
MgO	0.82	0.90	0.84	0.88	0.91	0.88	0.81
CaO	3.86	3.93	4.51	4.52	4.54	3.76	3.89
Na2O	0.18	0.14	0.15	0.10	0.07	0.11	0.09
K2O	3.06	2.92	2.66	2.59	2.52	2.83	2.84
Total	89.69	91.45	88.50	89.66	88.39	87.77	88.43
Atoms per formula unit (apfu)							
Si	29.588	29.664	29.106	29.235	29.136	29.661	29.691
Al	6.412	6.337	6.892	6.761	6.861	6.340	6.308
Mg	0.524	0.563	0.545	0.562	0.590	0.573	0.524
Ca	1.772	1.766	2.103	2.076	2.116	1.760	1.808
Na	0.150	0.114	0.127	0.083	0.059	0.093	0.076
K	1.672	1.562	1.476	1.416	1.398	1.577	1.571

The effect of milling on Na-exchanged clinoptilolite particles, as observed by the laser diffraction particle size analyzer, is shown in Figure 4. The results indicate that the tuff has a grain size ranging from approximately 0.6 μm to 200 μm. Clinoptilolite particles are multimodally distributed, with the following main peaks: from 0.5 to 1 μm, from 1.5 to 4.5 μm, from 5 to 45 μm, and from 65 to 150 μm. The grains with sizes between 5 and 45 μm are the most dominant.

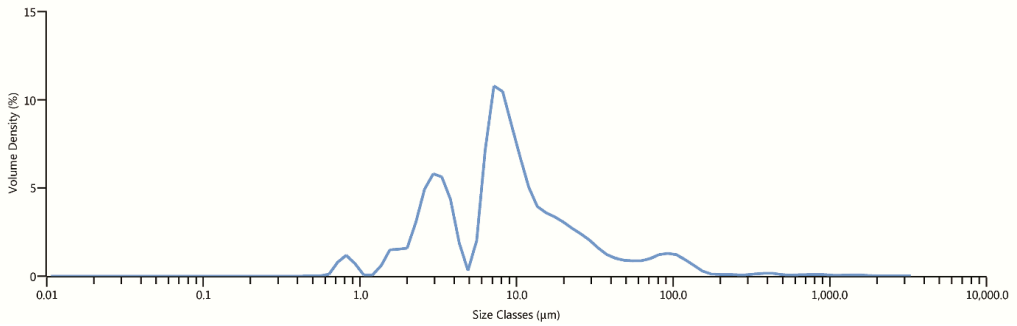

Figure 4. Mie-sizing of tribo-activated Na-exchanged clinoptilolite.

The distribution of particles smaller than 5 μm in the Na-exchanged and tribo-activated clinoptilolite was obtained using the Dynamic Light Scattering (DLS) technique. The correlation function provides a mathematical description of the fluctuations of the scattered light. This function is utilized to assess the quality of the analyses (Figure S1). The primary parameters influencing data quality are the average hydrodynamic diameter of the particles (effective diameter) and the width of their distribution, known as polydispersity (Table S2). Figure S1 presents the scattering intensity correlation function of tribo-activated clinoptilolite water solutions at three equal concentrations and a scattering angle of 90°. The continuous lines represent the best non-linear least-squares fits obtained under the assumption of a multimodal decay of correlations.

After determining the mean particle diameter and polydispersity values, these were fitted to a lognormal distribution representing the size distribution. They interpolated both cumulative and differential results at 5% intervals (Figure S2a). The cumulative distribution function of a random

 doi:10.20944/preprints202503.1874.v1

variable describes the distribution of that variable. Multimodal particle size distributions are established using a numerical algorithm and Mie theory. The particles were measured in the 100 to 5000 nm range, exhibiting a bimodal size distribution (Figure S2b). The finer particles display a broad size distribution in the 240–290 nm range, with a peak (average) near 260 nm. Large particles of tribo-activated clinoptilolite are observed with a distribution that has a high-intensity peak around 1600 nm. According to the results, the larger particles have an average effective diameter of 1696.6 nm and a narrow size distribution range from 1600 to 1800 nm (Table S2).

The specific surface area of the Na-exchanged and tribo-activated clinoptilolite was calculated using the Brunauer–Emmett–Teller (BET) method. Results are presented in Figure S3. The total pore volume is 0.051 cm^2/g, and the surface area is 24.2 m^2/g.

3.2. Heavy Metal Bioaccumulation

Table 3 presents the results of Cd bioaccumulation in the livers, kidneys, and feces of the animals studied in the CDw and CDwZ trials. A statistically significant accumulation ($p < 0.0001$) of Cd^{2+} was noted in both groups' targeted organs and feces compared to the baseline day. A significant reduction in liver accumulation ($p < 0.001$) was observed in the CDwZ animals, ranging from 19% on day 15 to 48% on day 45 compared to the findings from the CDw group. In the kidneys, the reduction varied from 26% to 61% over the same period (Table 3). The amount of Cd^{2+} absorbed by the modified clinoptilolite and excreted in the feces rose from 28% to 36% in animals from the zeolite +Cd group. This increase in Cd excretion indicates that zeolite could effectively aid in removing about 36% of the Cd through feces.

Table 3. The cadmium levels in the liver, kidneys, and feces (mg/kg dry weight) of the tested animals from the two experimental groups.

Days	Organs					
	CDw ($\bar{x}$±SD)			CDwZ ($\bar{x}$±SD)		
	Liver	Kidneys	Feces	Liver	Kidneys	Feces
0	0.3±0.1	0.2±0.1	0	0.3±0.1	0.2±0.1	0
15	56.2±1.1^{a,d}	53.1±1.8^{a}	113.0±2.8^{a}	44.2±1.6^{a}	39.1±0.9^{a}	156.0±3.2^{a}
30	96.0±3.6^{a,b,d}	104.0±12.6 ^{a,b}	153.0±13.4^{a,b,d}	78.0±12.1^{a,b}	74.6±11.8^{a,b}	200.0±22.1^{a,b}
45	173.0±11.9^{a,c,d}	260.0±23.1 ^{a,b,c}	177.0±13.1^{a,b,c,d}	90.0±12.3^{a,b,c}	100.0±12.4^{a,b,c}	276.0±22.6^{a,b,c}

Values marked with different superscript letters indicate a significant difference between groups at each time point: (a) between day 0 and days 15, 30, and 45; (b) between day 15 and days 30 and 45; (c) between day 30 and day 45; (d) between the CDw and CDwZ groups at the same time point. The values a, b, c, and d are significant at $p<0.0001$.

3.3. Growth Rate

Figure 5 shows the growth trends in mouse body mass observed during each trial. By the end of the experiment, all experimental mice exhibited an increase in weight, although the magnitude of the increase varied among groups. The most significant percentage increase in body weight was recorded in the zeolite-supplemented groups: 41.68% for Z and 42.52% for CDwZ. The control group followed with a weight gain of 37.34%, while the CDw group experienced the lowest weight gain at 22.0%. All mice supplemented with zeolites (groups Z and CDwZ) exhibited weight loss on days 15 and 30, respectively, followed by a statistically significant ($p < 0.0001$) and notable increase. Cd intoxication (CDw group) significantly reduced the growth rates of laboratory mice, resulting in an overall decrease in body mass of 12.89% by day 45 ($p < 0.001$) compared to the control group. After administering clinoptilolite, the CDwZ group demonstrated a statistically significant increase in body weight at the 15th and 45th experimental time points compared to the control group ($p < 0.05$).

 doi:10.20944/preprints202503.1874.v1

Notably, on day 45, the average weight difference between the CDw and CDwZ groups was about 5.0 g, representing a 15% variation.

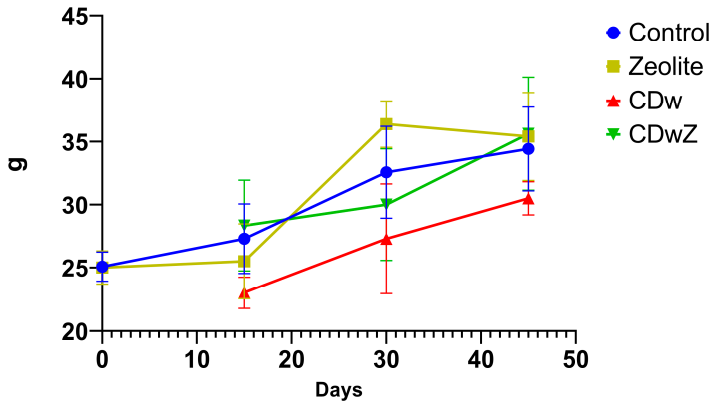

Figure 5. Changes in body weight (g) of laboratory mice (mean ± SD) related to experiments.

3.4. Organ Index Changes

Overall, both liver and kidney indices exhibited similar patterns of change throughout the experiment. The liver index for the Cd-exposed group (CDw) was significantly lower ($p < 0.0001$) on day 45 compared to the control group on the same day (Figure 6a). Additionally, the group exposed to Cd and supplemented with clinoptilolite (CdwZ) demonstrated the most effective remedial action on days 30 and 45, as their liver index returned to normal levels, aligning with those of the control group, with no statistically significant difference. As shown in Figure 6b, the kidney index of the CDw group on day 45 was significantly lower ($p < 0.001$) than that of the control group on day 0. In contrast, the kidney indices in the zeolite group did not reveal any significant differences compared to the control group. The harmful effects of Cd and the beneficial effects of zeolite become evident after 45 days.

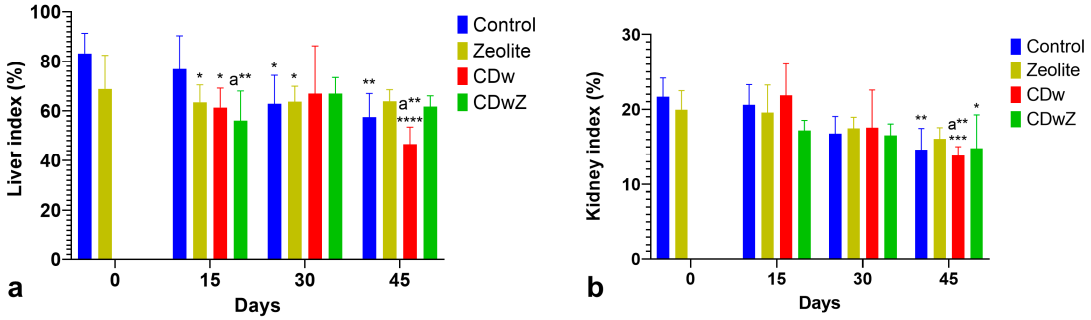

Figure 6. The liver index (a) and kidney index (b) for different experimental groups. The data are presented as mean ± SD. Values marked with asterisks indicate significant differences from the control group on day 0 (*$p < 0.05$, **$p < 0.01$, ***$p < 0.001$, and ****$p < 0.0001$). Superscripted values denote significant differences between the control group and other groups at the same time point.

3.5. Hematology

The results of the hematological analyses conducted during the sub-chronic experiments, both with and without clinoptilolite supplementation, are presented in Table 4. The study showed that the WBC and MO count leucogram markers exhibited significantly elevated levels ($p < 0.05$) in Cd-intoxicated mice compared to those not exposed to Cd from the control and zeolite-supplemented groups. Administering clinoptilolite to Cd-intoxicated mice resulted in a significant decrease ($p <$

 doi:10.20944/preprints202503.1874.v1

0.05) in the observed WBC, particularly in MO, compared to mice treated with Cd alone (Table 4). Among the erythrogram markers, Hgb, RBC, and Hct values showed a negative effect due to Cd intoxication after the trial, indicating a significant decrease compared to control day 0 ($p \leq 0.05$). The erythrogram indicators suggest the presence of hypochromic microcytic anemia resulting from Cd intoxication. Clinoptilolite supplementation mitigated the adverse effects of Cd, with the mice in the CDwZ group returning to normal erythrogram levels by day 15 and maintaining those levels until the end.

Table 4. The impact of Cd-exposure and clinoptilolite supplementation on hematological parameters in the tested laboratory mice during the sub-chronic experiments. The data are presented as means ±SD with N =32 for all experimental groups.

Parameters	**WBC** (g/L)				**LYM** (10^9/L)				**GR** (10^9/L)			
Groups / Days	**C**	**Z**	**CDw**	**CDwZ**	**C**	**Z**	**CDw**	**CDwZ**	**C**	**Z**	**CDw**	**CDwZ**
0	4.3± 1.7	4.3± 1.7	-	-	3.1± 1.2	3.2± 1.2	-	-	2.2± 0.8	2.6± 0.9	-	-
15	3.7± 1.5	3.6± 1.7	9.6± 1.9 ^{b,c}	4.6± 2.0	3.8± 0.8	2.1± 1.2	3.8± 1.2	2.2± 1.3	1.5± 0.4	1.1± 0.5	1.3± 0.3	0.8± 0.5
30	6.0± 1.3	7.2± 2.2	11.7± 2.5 ^{b,c}	6.0± 1.3^{c}	3.5± 1.4	3.8± 1.5	2.5± 1.8	2.8± 1.4	2.1± 0.7	2.7± 0.6*	1.0± 0.6 ^{b}	1.5± 0.7*
45	6.6± 3.2	7.8± 2.1*	8.1± 3.1	10.1± 7.4*	4.2± 2.7	4.4± 1.4	3.3± 2.5	4.2± 1.0	4.0± 2.9*	2.7± 0.8*	1.9± 1.5	3.2± 1.2^{*a}
	MO (10^9/L)				**RBC** (10^{12}/L)				**Hb** (g/L)			
0	2.6± 0.14	2.8± 0.19	-	-	3.3± 1.3	3.7± 1.0	-	-	69.6± 22.1	68.3±19.8	-	-
15	1.1± 0.03	1.0± 0.05	12.9± 0.22 ^{b}	2.1± 0.06^{b}	3.7± 0.6	3.4± 0.5	2.3± 1.5	5.6± 1.2	54.4± 12.9	70.0± 43.5	36.3± 24.0 ^{b,c}	45.0± 5.9
30	2.6± 0.14	0.9± 0.01	10.4± 0.62 ^{b}	1.7± 0.03^{b}	5.3± 2.0	3.9± 1.4	3.1± 1.9*	5.7± 3.8	81.1± 29.5	79.3±2 8.3	28.3± 16.6 ^{b,c}	56.0± 25.2
45	4.1± 0.26	1.1± 0.07	12.4± 0.18^{*a}	2.2± 0.06	.9± 2.6*	4.2± 1.3	1.8± 1.2^{*a,b,c}	5.3± 3.5	82.9± 37.3	89.3± 10.6	22.7± 11.7* ^{b}	69.9± 14.4 ^{b}
	Hct (L/L)				**MCV** (fL)				**MCH** (pg)			
0	0.25± 0.09	0.24± 0.09	-	-	46.8± 1.6	46.8± 1.6	-	-	15.3± 1.0	15.3± 1.0	-	-
15	0.26± 0.08	0.19± 0.06	0.22± 0.06	0.12± 0.07	48.7± 5.4	48.8± 6.5	42.2± 2.4^{c}	50.0± 4.4	15.6± 1.5	15.1± 1.6	12.5± 0.3 ^{b,c}	15.5± 1.0^{c}

 doi:10.20944/preprints202503.1874.v1

30	0.25±	0.19±	0.23±	0.27±	46.8±	48.2±	41.7±	44.4±	15.3±	14.0±	13.0±	13.7±
	0.12	0.07	0.14	0.09	1.6	3.0	4.1	3.0	1.0	1.2	1.1 [b]	0.7
45	0.26±	0.21±	0.24±	0.07±	44.0±	50.4±	44.7±	41.9±	14.0±	14.9±	13.5±	14.2±
	011	0.05	0.15	0.04[a]	4.5	1.3	3.5	2.7[b]	1.8	0.5	3.0	1.3

The asterisk indicates statistically significant differences ($p < 0.001$) compared to the control day 0 within the column. Similarly, the data marked with (a) indicate statistically significant differences ($p < 0.05$) when comparing day 45 to day 30 within the same column. The data marked with a (b) represent differences within a row compared to the control value. The data marked with a (c) represent differences ($p < 0.05$) within a row compared to the previous value.

3.6. Oxidative Stress

The activities of oxidant-antioxidant enzymes in liver and kidney tissues were significantly affected by Cd exposure, time factors, and their interaction. Figure 7 illustrates the hepatic and renal sub-chronic toxicity of Cd, assessed by measuring GSH and MDA levels. Compared to the control group, MDA levels were significantly elevated after Cd supplementation ($p < 0.05$). As shown in Figure 7a, liver and kidney MDA contents increased significantly in response to $Cd(NO_3)_2$ treatment by 41.38% and 40.79%, respectively, on day 15, compared to those in the control group ($p < 0.01$). Conversely, levels of the antioxidant enzyme GSH were significantly reduced ($p < 0.05$) (Figure 7b). A strong inverse correlation between MDA and GSH levels was observed ($p < 0.001$, $r = –0.947$). Liver and kidney GSH levels were notably reduced on day 15 after $Cd(NO_3)_2$ treatment by 185.71% and 235.04%, respectively. Consequently, Cd intoxication caused an imbalance in hepatic and renal oxidation, resulting in oxidative stress. Treatment combining Cd and clinoptilolite significantly increased GSH levels in the liver and kidneys compared to the Cd-only group ($p < 0.05$) but did not reach control levels. MDA levels decreased but remained elevated compared to controls. On day 45, MDA and GSH levels were still below controls, with no significant statistical differences observed.

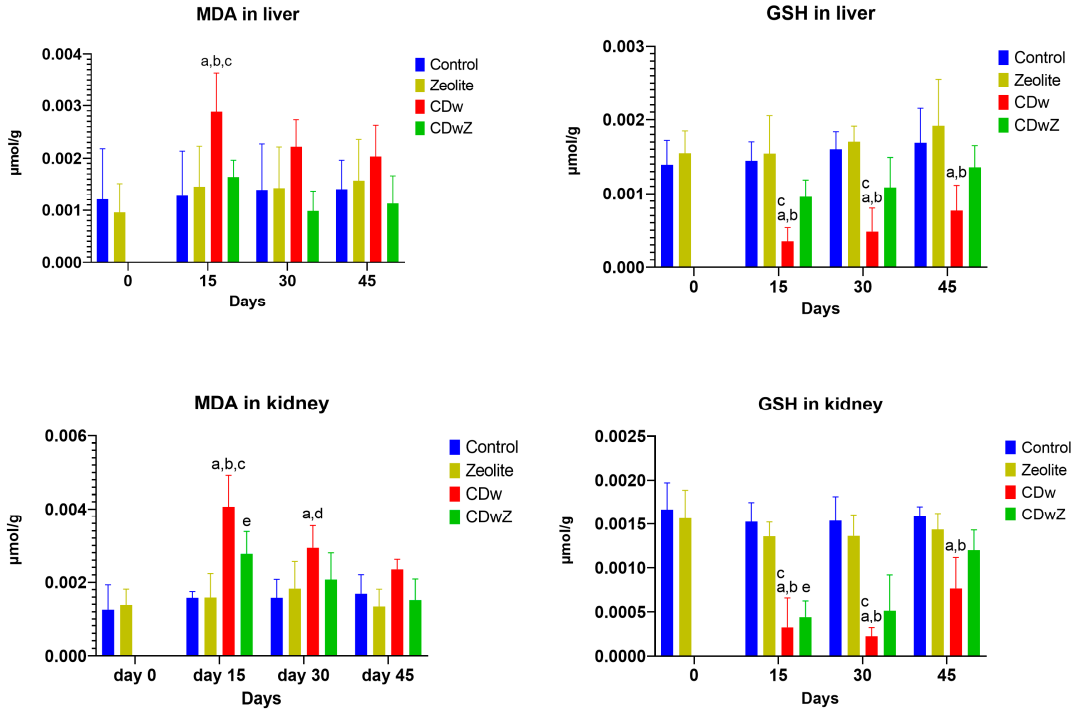

Figure 7. The levels of MDA (a) and GSH (b) in the liver and kidneys of mice during various trials. Asterisks indicate statistically significant differences in the CDw-mice values compared to all control time points. Superscript (a) denotes significant differences between the CDw-mice values and all time points in the zeolite

 doi:10.20944/preprints202503.1874.v1

group, while superscript (b) highlights differences between the CDw-mice and all other time points for the CDwZ group (* p<0.05, ** p<0.01, *** p<0.001, **** p<0.0001).

3.7. Micronucleus Test

Figure 8 illustrates the in vivo micronucleus test results, which evaluated genotoxic stress in the red blood cells of the experimental animals. The frequency of micronuclei in mouse erythrocytes significantly increased (p<0.0001) over time following exposure to in the CDw group. In contrast, no increased levels of micronuclei were detected after zeolite supplementation during the CDwZ experiment, and they remained stable near control frequencies.

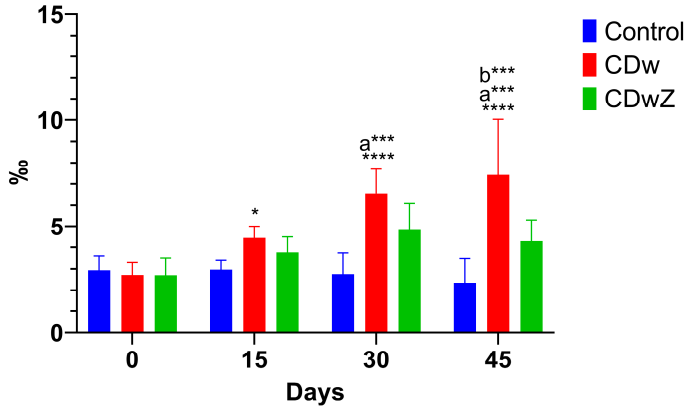

Figure 8. Frequency of micronuclei (MN/1000) in the erythrocytes of mice from the Control, CDw, and CDwZ groups. Asterisks indicate statistically significant differences between the control and other experimental time points. Superscript (a) highlights significant differences between the marked values and other CDw-mice values, while superscript (b) denotes significant differences between the indicated CDw-mice values and CDwZ-mice values. (*p<0.05, ***p<0.001, ****p<0.0001).

4. Discussion

4.1. Sorption Properties of Modified Natural Zeolite-Clinoptilolite

Natural zeolites are a unique group of minerals. Numerous studies on these silicate minerals exist, but none specifically focus on natural zeolites. Certain types, such as clinoptilolite, show significant potential due to their high sorption capacity and extensive deposits in various countries. Bulgaria is among the countries with vast reserves of high-quality clinoptilolites [12–14]. The structural properties of this mineral determine its specific characteristics regarding ion exchange and selective sorption [2]. Modifying zeolite surfaces by incorporating specific surfactants has improved the ion exchange capacity, thus facilitating the removal of cations, anions, and various organic compounds [62]. This process is crucial for enhancing the sorption capacity of these minerals. According to [54], Na-exchanged clinoptilolite has a greater Cd exchange capacity than the natural form.

Clinoptilolites are increasingly recognized as effective agents for alleviating the harmful effects of heavy metal pollution. Due to the mineral's unique physicochemical properties, high ion exchange capacity, and adsorption capabilities, zeolites offer significant potential for decontamination and reducing the metal burden in mice [17]. Clinoptilolite is regarded as the only safe zeolite material used in medical applications due to its well-documented positive effects on animal and human health and performance [63]. The European Food Safety Authority (EFSA) published a favorable evaluation of the integrity and safety of natural zeolite clinoptilolite for both animal and human consumption [64]. Additionally, EFSA provided data demonstrating that clinoptilolite poses no toxicity for animal feed, even at high doses (10000 mg/kg), due to its exceptional chemical properties and thermal

 doi:10.20944/preprints202503.1874.v1

stability. According to EU Regulation 744/2012 [51], the clinoptilolite tuff from the Beli Plast deposit is considered suitable for use as a feed additive because the levels of Pb and Cd are lower than the maximum permissible values of 60 ppm and 5 ppm, respectively, and the concentration of As is below the detection limit. Consequently, it could be used as a sorbent for detoxification purposes. The potential adverse effects of the modified natural clinoptilolite used in this study on normal physiological processes in animals have been previously assessed, showing no evidence of pharmacological intoxication or unusual behavior [65]. The current results indicate that all animals receiving a clinoptilolite supplement survived the experiment. Mice gained body mass and displayed good activity and vitality. No differences were found in the physiological parameters examined between the mice supplemented with clinoptilolite and the control group. The research findings were entirely attributed to Cd exposure and the sorption capacity of the zeolite under equilibrium conditions, free from any influence by other stressors that could affect the results.

Limited research has documented various in vivo effects of clinoptilolite focused on Pb detoxification, including its antioxidant, hemostatic, immunomodulatory, and detoxification properties [18–20,66]. In the current study, the observed biological response in mice, indicated by the reduction in Cd accumulation in the liver, kidneys, and feces, is likely due to the porous nature of clinoptilolite and its ability to retain exchangeable cations. The aluminum (Al) ion in the tetrahedron of oxygen atoms substitutes Al^{3+} for Si^{4+}, increasing the lattice's negative charge [11]. This attracts positive cations present in physiological environments, such as sodium (Na), potassium (K), and calcium (Ca), creating a strong electrostatic field on the internal surface. Given their higher binding affinity for the clinoptilolite lattice, these cations can be exchanged to modify pore size or adsorption characteristics in an aqueous medium [11,66,67]. All clinoptilolite modifications rely on these principles, as pore size plays a crucial role in Na^{+}, K^{+}, or Ca^{++} exchange with cations like Pb^{2+}, Cd^{2+}, and Zn^{2+} in solutions [67]. It is important to note that clinoptilolite shows a strong affinity for heavy metal cations, including Cd, lead (Pb), manganese (Mn), zinc (Zn), chromium (Cr), and arsenic (As) [63,68–72]. The theoretical internal surface area of clinoptilolite pores available for cation exchange is extensive and significant concerning the observed biological effects of clinoptilolite. Estimates range from 10 to 300 m^2/g [73]. Similarly, the estimated surface area of the modified zeolite tested in this study is 24.2 m^2/g, slightly lower than the values (30 m^2/g) reported for natural tribomechanical-activated clinoptilolites [62].

In both humans and animals, clinoptilolite interacts within the acidic intestinal environment. The ability of fluids to reach the zeolitic surface while passing through the gastrointestinal tract relies on their specific characteristics, including the particle size of the zeolitic material, crystallite size, degree of aggregation, and the porosity of individual particles [16,74]. They significantly impact the zeolite's ion exchange, adsorption, and catalytic properties. The SiO_2/Al_2O_3 ratio in zeolites is an important indicator of their acid stability. A higher SiO_2/Al_2O_3 ratio correlates with increased acid stability of the zeolites [17]. The Na-exchanged and tribomehanical-activated clinoptilolite used in this study possesses the necessary characteristics (chemical content, grain size, multimodally distributed clinoptilolite particles, high SiO_2/Al_2O_3 ratio), highlighting its suitability as a reliable sorbent for Cd^{2+}.

Numerous studies have evaluated clinoptilolites' ability to remove heavy metals in an *in vitro* model that simulates the conditions of the stomach and small intestine. The structure and sequestration capability of clinoptilolite remains unaffected by pH and dietary mixtures, indicating that the mineral can be effectively applied in these biological contexts. As employed in the present study, the concurrent administration of clinoptilolite and metal has been demonstrated in numerous studies to be efficacious when metals and clinoptilolite are combined [62,75–77].

4.1. Cadmium Toxicity and Bioaccumulation

The present study supports the previously observed effects of clinoptilolite administration on heavy metal concentration profiles in rodent organisms [16–18,62,65]. However, this research marks the first investigation into the effects of a specially modified clinoptilolite with enhanced Cd^{2+}

 doi:10.20944/preprints202503.1874.v1

exchange capacity, used as a dietary supplement, on Cd-exposed animals. Cd has a long half-life [26] and accumulates in the liver and kidneys, potentially causing severe hepatotoxicity and nephrotoxicity (27, 28). Its absorption increases metallothionein (MT) synthesis, forming Cd-MT complexes. Cd toxicity causes hepatocyte death, transporting these complexes to the kidneys [78], where they accumulate and heighten chronic toxicity [79]. Once reabsorbed, Cd degrades into more toxic free and bound forms, with free Cd damaging renal tubular epithelial cells significantly [80,81].

The observed decline in Cd bioaccumulation in the liver, kidneys, and excreted feces of animals from the CDwZ group demonstrated the effectiveness of the modified natural clinoptilolite's chemical composition and morphological structure in enhancing Cd sorption capacity. On day 45, clinoptilolite reduced the Cd content in liver tissues by about 50%, in kidney tissues by 60%, and in feces by 36%. The concentration ratio Cd45/Cd15 is often called the bioaccumulation coefficient. The bioaccumulation coefficients in exposed and unsupplemented mice are significantly higher than in exposed and supplemented mice [17]. For the CDw group, the coefficients are 3.07 for the liver, 4.90 for the kidney, and 1.54 for the feces. For CDwZ mice, they are 2.04, 2.55, and 1.77, respectively (Table 3). A significant reduction of this coefficient, particularly for the kidney, was established. This indicates that the modified natural clinoptilolite significantly reduces the Cd levels in the blood by acting within the gastrointestinal tract and considerably decreasing the Cd absorption by the mucosa. This further demonstrates the significant reduction in Cd bioaccumulation resulting from the ion exchange capacity of the Na-activated sorbent. In mice exposed to Pb, a modified natural clinoptilolite sorbent, KLS-10-MA, decreased Pb accumulation in the intestine by over 70% [17,19]. Previous studies have demonstrated that Bulgarian clinoptilolites from deposits in the Eastern Rhodopes [17–19] support the organism's normal physiological state during chronic heavy metal intoxication by absorbing significant Pb^{2+} amounts. Results from several authors indicate that the Na-enriched form of modified clinoptilolite has the highest static ion exchangeability for Pb^{2+}, Cd^{2+}, NH_4^+, and others [75–77]. Therefore, the modification that has been undergone can be regarded as successful for detoxification.

However, further and more detailed laboratory research is necessary to clarify the effects of varying concentrations of Cd and clinoptilolite. This will enhance the understanding of this mineral's role as a sorbent when used as an animal food additive.

4.2. Growth Rate

Body mass gain is a reliable indicator of an animal's health status. The changes in this parameter after consuming zeolite-enriched food have been well-established in animal husbandry for many years [83–86]. Studies regarding the detoxification capacity of natural clinoptilolite following sub-chronic Pb intoxication have also shown significant alterations in body weight [17]. However, the degree of enhancement effects is influenced by the type of zeolite used, its purity, physicochemical properties, and the level of dietary supplementation. [83]. Administering clinoptilolite as a food additive can significantly enhance the overall physiological condition of the organism. The decrease in body mass due to chronic Cd intoxication is notably more pronounced compared to cases where clinoptilolite was included in the diet. The current finding that the body mass of the experimental mice increased by about 15% in the presence of a clinoptilolite additive is consistent with previous results obtained from clinoptilolites from various deposits [83–85].

4.3. Hematology

Hematological parameters in mice indicate environmental and toxic stressors, making the hematopoietic system essential for assessing toxicity in small mammals [86,87]. Hb, RBCs, Hct, and WBCs are sensitive indicators of animal health, reflecting oxygen-carrying capacity and immune system status [88]. Hb and RBC erythrogram parameters are crucial for diagnosing anemia, often observed in Pb and Cd intoxication cases [89].

The study identified hypochromic microcytic anemia in Cd-exposed mice, aligning with previous research [31,90,91]. Cd intoxication resulted in decreased RBC counts, Hb, Hct, and

 doi:10.20944/preprints202503.1874.v1

increased total WBCs [31]. The microcytic anemia observed can lead to hemolysis due to RBC deformation [90], iron deficiency from competition in duodenal absorption [91], and renal anemia as a result of reduced erythropoietin (EPO) production [92]. After exposure, Cd^{2+} was attached to RBC membranes and plasma albumin, stimulating the production of MTs and ROS, which leads to oxidative stress in RBCs. [93,94]. RBC indices reflect cell characteristics and are stable measures. Cd exposure altered RBC membrane permeability and reduced intestinal iron absorption due to mucosal lesions, leading to lower hematocrit levels [95–97]. Increased WBC counts after Cd exposure may result from heightened free radicals, reduced antioxidant activity, immune response suppression, and systemic inflammation [98].

Supplementing the diet with zeolite helped alleviate the adverse effects of Cd on the measured hematological parameters (Table 2). The results reveal that the primary function of zeolite supplements is to reduce the harmful impacts of physiological stress by lowering the overall levels of Cd [99]. Zeolites, which function as ion exchangers, also contribute to specific biochemical transformations, stabilize animal homeostasis, and improve nutrient conversion, potentially raising RBC and Hb levels [20]. Clinoptilolite has low solubility in water at physiological pH and is not absorbed into circulation from the gut [100]. Therefore, any effects on hematopoiesis are likely due to indirect mechanisms initiated in the gut. [101] studied the effects of natural clinoptilolite on mice's hematopoiesis, serum electrolytes, and organ function. During 2 weeks of supplementation, a slight increase in Na levels was noted in mice on a zeolite-rich diet. No other changes were observed in serum chemistry or peripheral blood levels of RBC, Hb, thrombocytes, MCV, and MCH. Clinoptilolite's ion exchange properties can affect gastrointestinal secretions' pH and buffering capacity, improve iron absorption, bind heavy metal ions, and influence intestinal microflora [102]. As a result, the supply of clinoptilolite may have delayed or long-lasting effects on the erythron and could trigger a systemic lympho-hematopoietic response.

The scientific literature has documented the positive effects of various zeolites on blood parameters for over a decade. However, data on their ion-exchange properties regarding chronic heavy metal intoxication and their impact on hematological parameters in mammals remain limited. [20] demonstrated that clinoptilolite materials directly detoxify *in vivo*, restoring erythrocytes in rats after organophosphate poisoning. [18] reported a 1.5-fold increase in the percentage of normal erythrocytes in the erythrogram of laboratory mice chronically exposed to Pb following zeolite supplementation. However, studies on other mammalian species have shown that clinoptilolite can effectively counteract Cd toxicity in pigs. Clinoptilolite supplementation prevented cadmium-induced iron deficiency anemia in growing swine receiving 150 ppm $CdCl_2$ [103]. In this context, the present study concerning the Cd-detoxification capacity of zeolites in a sub-chronic experiment and its impact on hematological parameters in small mammals represents a first step. The long-term effects of clinoptilolite on biological systems, including its potential toxicity and biocompatibility, must be more thoroughly investigated.

4.4. Oxidative Stress

Oxidative stress significantly contributes to Cd-induced organ toxicity and carcinogenicity [104]. Although Cd lacks redox potential, it raises intracellular ROS levels, causing oxidative damage to lipids, proteins, and DNA [104,105]. The liver is crucial in detoxifying drugs and chemicals [106].

The obtained data confirm the results of previous studies [107,108] on chronic Cd intoxication. This research has shown that Cd intoxication decreases the activity of antioxidant enzyme systems. This is marked by a substantial drop in GSH levels and a significant rise in MDA levels in the liver and kidneys, resulting in cellular oxidative stress. Higher concentrations of endogenous GSH were found in the liver compared to the kidney. However, the liver is highly vulnerable to oxidative damage caused by GSH depletion. When hepatic GSH levels decrease below 20% of normal, the cell's defense against oxidative stress is impaired, potentially causing hepatic injury [109]. In rats, a decrease in hepatic GSH levels (27-34%) indicates Cd-induced hepatic injury [20]. Previous studies have shown similar GSH depletion *in vitro* and *in vivo* after Cd intoxication [20,110]. While

 doi:10.20944/preprints202503.1874.v1

mechanisms exist to neutralize free radicals and maintain cellular redox balance, Cd disrupts this equilibrium, leading to secondary hepatic injuries, such as inflammation, apoptosis, and liver dysfunction [111–113]. Although GSH levels remained low on day 45, the MDA levels in the liver and kidneys of both CDw and CDwZ groups rose after 30 days. A strong correlation existed between MDA and GSH levels, indicating a reciprocal relationship. This suggests that lipid peroxidation, indicated by MDA, increases when GSH levels in liver and kidney cells decrease. The current results are partially consistent with a study by [114] comparing the Pb—and Cd-induced oxidative stress profiles in the liver and kidneys of sub-chronically exposed mice. In the kidneys of Cd-exposed mice, the highest accumulation of MDA was detected, along with a 1.5-fold GSH depletion. According to the authors, Cd intoxication causes more oxidative damage in the kidneys due to the bioaccumulation profiles of the two metals.

Suppressing oxidative stress by increasing antioxidant capacity mitigates the pathological changes induced by Cd exposure [38]. Current research suggests that sub-chronic Cd exposure modified the liver's antioxidant defense systems, which zeolite could help mitigate by reducing elevated MDA levels due to the depletion of GSH. Daily supplementation of modified natural clinoptilolite enhanced antioxidant capacity. Similar results are obtained by [20], which shows that micronized clinoptilolite supplementation in hepatectomized rats improved MDA levels and liver tissue antioxidant mechanisms. Cu-Zn superoxide dismutase (SOD) and GSH activity were higher in rats supplemented with clinoptilolite. Extended supplementation also boosted the activities of glutathione peroxidase, catalase, total SOD, and total antioxidant capacity [115]. In mice treated with doxorubicin, micronized clinoptilolite effectively countered liver lipid peroxidation [20]. Clinoptilolite has positive immunomodulatory effects due to its interactions with microfold cells (M-cells) in the intestine [116]. M-cells can uptake nano- and submicron-particles, changing the cell's redox homeostasis. Clinoptilolite particles can be retained by M-cells, acting locally on the tissue and not entering the bloodstream. This communication between M-cells induced by clinoptilolite enhances the immune response, stimulating IgA-producing B lymphocytes as a defensive mechanism against toxicants [117]. Further studies are required to fully clarify the issue, including more detailed investigations into sub-chronic Cd doses and longer-term experiments. The data suggest that sub-chronic Cd exposure modified the liver's antioxidant defense systems, which zeolite could help mitigate by reducing elevated MDA levels due to the depletion of GSH.

4.5. Genotoxic Effects

Cd causes toxicity by altering gene expression, inhibiting DNA repair, and interfering with apoptosis. It is associated with increased frequencies of micronuclei (MNs) and other indicators of DNA damage, significantly raising the number of micronucleated polychromatic erythrocytes [40,118]. MNs are evidence of mutagen-induced chromosomal aberrations, resulting from acentric fragments and lagging chromosomes in anaphase [40]. Cd may exert strong indirect genotoxic effects by interfering with DNA repair, leading to accumulated and stable DNA damage [119].

The current MN test demonstrates a parallel link between Cd levels in the body and heightened MN frequency during sub-chronic Cd treatment, indicating that cytotoxicity depends on Cd concentration in the internal organs and erythrocytes. Cd is known to be genotoxic even at low doses, including micromolar concentrations, with these effects appearing before any other observable physiological damage [119,120], resulting in chromosomal damage, as measured by the MN test. These effects increase linearly with dose [119,120]. After zeolite supplementation, a statistically significant difference was observed on day 45 between CDw and CDwZ mice. The reduction of Cd impact in the zeolite-supplemented mice led to decreased heavy metal loading, as demonstrated by ICP-MS spectrometric analysis (Table 3) and the resulting prevention in MNs formation.

More data is needed on the effect of zeolites on MN frequencies. Previous studies have shown that modified natural clinoptilolite KLS-10-MA from Bulgarian deposits, used as a Pb adsorber in mice, did not cause damage to the chromosomal structure and was effective [19]. Further investigations on the sensitivity of DNA stability to Cd intoxication could help to understand

 doi:10.20944/preprints202503.1874.v1

genomic damage better and reveal the dependence between oxidative stress and genotoxic effects. The current results confirm the induction of MNs by low Cd doses and demonstrate the apparent genoprotective effect of the tested clinoptilolite as an *in vivo* sorbent of Cd^{2+} in the animal intestine.

5. Conclusions

The zeolitized tuff from the Bulgarian deposit contains a mineral assemblage that renders it safe and suitable for feed additives, as it has lower levels of Pb, Cd, and As than the maximum permissible limits. The natural clinoptilolite was transformed into Na-exchanged clinoptilolite that was tribe-activated, resulting in an enhanced capacity for Cd^{2+} exchange. The environmentally relevant doses of Cd used in exposure experiments lead to intoxication, resulting in significant bioaccumulation, hypochromic microcytic anemia, oxidative stress, and genotoxic damage. The 45-day *in vivo* supplementation with Na-modified natural clinoptilolite demonstrated a clear protective effect by reducing Cd bioaccumulation, restoring hematological indices, normalizing antioxidant levels, and preventing the induction of MNs. The protective effect of clinoptilolite may arise from its capacity to limit Cd absorption by the intestinal mucosa, prevent its entry into the bloodstream, and significantly decrease the physiological damage associated with sub-chronic Cd intoxication. These findings suggest a prerequisite and a potential long-term opportunity for such products to serve as cost-effective detoxifiers in Cd-contaminated areas.

Supplementary Materials: The following supporting information can be downloaded at Preprints.org, Figure S1: Correlation function at three measurements; Figure S2: Particle size distribution in water (a) and particle size multimodal distribution based on APD photodetector (b); Figure S3: The BET surface area and porosity analysis of the Na-exchanged and tribo-activated clinoptilolite; Table S1: Concentrations of selected trace elements in clinoptilolite tuffs from the studied deposits (in ppm); Table S2: Results from the statistics data at DLS measurements.

Author Contributions: Conceptualization, M.B. and Y.T.; methodology, M.B. and Y.T.; formal analysis, T.C.; investigation, I.A.; P.O.;L.T.;R.R.; data curation, M.B.;Y.T.;T.C.; writing—original draft preparation, M.B.; Y.T.; writing—review and editing, T.C.; visualization, Y. T. and T.C.; supervision, M.B.;.

Funding: This research was funded by the Bulgarian National Science Fund, Ministry of Education and Science, grant number No. KP-06-PN44/3.

Institutional Review Board Statement: The Institute of Biodiversity and Ecosystem Research Ethics Committee has approved the animal study protocol, with protocol code 001/18.03.2024.

Informed Consent Statement: Not applicable.

Data Availability Statement: The original contributions presented in this study are included in the article and supplementary material. Further inquiries can be directed to the corresponding authors.

Conflicts of Interest: The authors declare no conflicts of interest. The funders had no role in the study's design, data collection, analysis, or interpretation, manuscript writing, or decision to publish the results.

References

1. Martinez-Morata, I.; Sobel, M.; Tellez-Plaza, M.; Navas-Acien, A.; Howe, C.G.; Sanchez, T.R. A State-of-the-Science Review on Metal Biomarkers. *Curr Environ Health Rep* **2023**, *10*, 215–249, doi:10.1007/s40572-023-00402-x.
2. Mumpton, F.A. *La Roca Magica*: Uses of Natural Zeolites in Agriculture and Industry. *Proceedings of the National Academy of Sciences* **1999**, *96*, 3463–3470, doi:10.1073/pnas.96.7.3463.
3. Bish, D.L.; Ming, D. Reviews in Mineralogy & Geochemistry: Occurrence, Properties, Applications. *Natural Zeolites* **2001**, *45*, 1–10.
4. Coombs, D.S.; Alberti, A.; Armbruster, T.; Artioli, G.; Colella, C.; Galli, E.; Grice, J.D.; Liebau, F.; Mandarino, J.A.; Minato, H.; et al. Recommended Nomenclature for Zeolite Minerals: Report of the Subcommittee on

 doi:10.20944/preprints202503.1874.v1

Zeolites of the International Mineralogical Association, Commission on New Minerals and Mineral Names. *Mineral Mag* **1998**, *62*, 533–571, doi:10.1180/002646198547800.

5. Doebelin, N.; Armbruster, T. Stepwise Dehydration and Change of Framework Topology in Cd-Exchanged Heulandite. *Microporous and Mesoporous Materials* **2003**, *61*, 85–103, doi:10.1016/S1387-1811(03)00358-5.
6. Merkle, A.B.; Slaughter, M. Determination and Refinement of the Structure of Heulandite. *American Mineralogist: Journal of Earth and Planetary Materials* **1968**, *53*, 1120–1138.
7. Alberti, A. The Crystal Structure of Two Clinoptilolites. *TMPM Tschermaks Mineralogische und Petrographische Mitteilungen* **1975**, *22*, 25–37, doi:10.1007/BF01081301.
8. Koyama, K.; Takeuchi, Y. Clinoptilolite: The Distribution of Potassium Atoms and Its Role in Thermal Stability. *Z Kristallogr Cryst Mater* **1977**, *145*, doi:10.1524/zkri.1977.145.16.216.
9. Carey, J.W.; Bish, D.L. Equilibrium in the Clinoptilolite-H 2 O System. *American Mineralogist* **1996**, *81*, 952–962, doi:10.2138/am-1996-7-817.
10. Armbruster, T.; Gunter, M.E. Stepwise Dehydration of Heulandite-Clinoptilolite from Succor Creek, Oregon, USA: A Single-Crystal X-Ray Study at 100 K. . *American Mineralogist* **1991**, *76*, 1872–1888.
11. Langella, A.; Pansini, M.; Cappelletti, P.; de Gennaro, B.; de' Gennaro, M.; Colella, C. Cu2+, Zn2+, Cd2+ and Pb2+ Exchange for Na+ in a Sedimentary Clinoptilolite, North Sardinia, Italy. *Microporous and Mesoporous Materials* **2000**, *37*, 337–343, doi:10.1016/S1387-1811(99)00276-0.
12. Aleksiev, B.; Djourova, E.G. On the Origin of Zeolite Rocks. . *C. R. Acad. Bulg. Sci.* **1975**, *28*, 517–520.
13. Aleksiev, B.; Djourova, E.G. Mordenite Zeolitites from the Northeastern Rhodopes. *Proceedings of the National Academy of Sciences* **1976**, *29*, 865–867.
14. Yanev, Y.; Cochemé, J.J.; Ivanova, R.; Grauby, O.; Burlet, E.; Pravchanska, R. Zeolites and Zeolitization of Acid Pyroclastic Rocks from Paroxysmal Paleogene Volcanism, Eastern Rhodopes, Bulgaria. *Neues Jahrbuch für Mineralogie - Abhandlungen* **2006**, *182*, 265–283, doi:10.1127/0077-7757/2006/0050.
15. Yanev, Y.; Ivanova, R. Mineral Chemistry of the Collision-Related Acid Paleogene Volcanic Rocks of the Eastern Rhodopes, Bulgaria. . *Geochemistry, Mineralogy and Petrology* **2010**, *48*, 39–65.
16. Dolanc, I.; Ferhatović Hamzić, L.; Orct, T.; Micek, V.; Šunić, I.; Jonjić, A.; Jurasović, J.; Missoni, S.; Čoklo, M.; Pavelić, S.K. The Impact of Long-Term Clinoptilolite Administration on the Concentration Profile of Metals in Rodent Organisms. *Biology (Basel)* **2023**, *12*, 193, doi:10.3390/biology12020193.
17. Beltcheva, M.; Metcheva, R.; Popov, N.; Teodorova, S.E.; Heredia-Rojas, J.A.; Rodríguez-de la Fuente, A.O.; Rodríguez-Flores, L.E.; Topashka-Ancheva, M. Modified Natural Clinoptilolite Detoxifies Small Mammal's Organism Loaded with Lead I. Lead Disposition and Kinetic Model for Lead Bioaccumulation. *Biol Trace Elem Res* **2012**, *147*, 180–188, doi:10.1007/s12011-011-9278-4.
18. Topashka-Ancheva, M.; Beltcheva, M.; Metcheva, R.; Rojas, J.A.H.; Rodriguez-De la Fuente, A.O.; Gerasimova, T.; Rodríguez-Flores, L.E.; Teodorova, S.E. Modified Natural Clinoptilolite Detoxifies Small Mammal's Organism Loaded with Lead II: Genetic, Cell, and Physiological Effects. *Biol Trace Elem Res* **2012**, *147*, 206–216, doi:10.1007/s12011-011-9289-1.
19. Metcheva R, B.M. Zeolites versus Lead Toxicity. *J Bioequivalence Bioavailab* **2015**, *07*, doi:10.4172/jbb.1000209.
20. Kraljević Pavelić, S.; Simović Medica, J.; Gumbarević, D.; Filošević, A.; Pržulj, N.; Pavelić, K. Critical Review on Zeolite Clinoptilolite Safety and Medical Applications in Vivo. *Front Pharmacol* **2018**, *9*, doi:10.3389/fphar.2018.01350.
21. Wu, Y.; Wu, Q.; Zhou, Y.; Ahmad, H.; Wang, T. Effects of Clinoptilolite on Growth Performance and Antioxidant Status in Broilers. *Biol Trace Elem Res* **2013**, *155*, 228–235, doi:10.1007/s12011-013-9777-6.
22. Montinaro, M.; Uberti, D.; Maccarinelli, G.; Bonini, S.A.; Ferrari-Toninelli, G.; Memo, M. Dietary Zeolite Supplementation Reduces Oxidative Damage and Plaque Generation in the Brain of an Alzheimer's Disease Mouse Model. *Life Sci* **2013**, *92*, 903–910, doi:10.1016/j.lfs.2013.03.008.
23. Trottier, B.; Athot, J.; Ricard, A.C.; Lafond, J. Maternal–Fetal Distribution of Cadmium in the Guinea Pig Following a Low Dose Inhalation Exposure. *Toxicol Lett* **2002**, *129*, 189–197, doi:10.1016/S0378-4274(02)00007-3.
24. Zhang, J.; Zheng, S.; Wang, S.; Liu, Q.; Xu, S. Cadmium-Induced Oxidative Stress Promotes Apoptosis and Necrosis through the Regulation of the MiR-216a-PI3K/AKT Axis in Common Carp Lymphocytes and Antagonized by Selenium. *Chemosphere* **2020**, *258*, 127341, doi:10.1016/j.chemosphere.2020.127341.

 doi:10.20944/preprints202503.1874.v1

25. Wang, C.; Nie, G.; Yang, F.; Chen, J.; Zhuang, Y.; Dai, X.; Liao, Z.; Yang, Z.; Cao, H.; Xing, C.; et al. Molybdenum and Cadmium Co-Induce Oxidative Stress and Apoptosis through Mitochondria-Mediated Pathway in Duck Renal Tubular Epithelial Cells. *J Hazard Mater* **2020**, *383*, 121157, doi:10.1016/j.jhazmat.2019.121157.
26. Wang, M.; Chen, Z.; Song, W.; Hong, D.; Huang, L.; Li, Y. A Review on Cadmium Exposure in the Population and Intervention Strategies Against Cadmium Toxicity. *Bull Environ Contam Toxicol* **2021**, *106*, 65–74, doi:10.1007/s00128-020-03088-1.
27. Zhang, H.; Reynolds, M. Cadmium Exposure in Living Organisms: A Short Review. *Science of The Total Environment* **2019**, *678*, 761–767, doi:10.1016/j.scitotenv.2019.04.395.
28. Genchi, G.; Sinicropi, M.S.; Lauria, G.; Carocci, A.; Catalano, A. The Effects of Cadmium Toxicity. *Int J Environ Res Public Health* **2020**, *17*, 3782, doi:10.3390/ijerph17113782.
29. Kandemir, F.M.; Caglayan, C.; Darendelioğlu, E.; Küçükler, S.; İzol, E.; Kandemir, Ö. Modulatory Effects of Carvacrol against Cadmium-Induced Hepatotoxicity and Nephrotoxicity by Molecular Targeting Regulation. *Life Sci* **2021**, *277*, 119610, doi:10.1016/j.lfs.2021.119610.
30. Klaassen, C.D.; Liu, J.; Diwan, B.A. Metallothionein Protection of Cadmium Toxicity. *Toxicol Appl Pharmacol* **2009**, *238*, 215–220, doi:10.1016/j.taap.2009.03.026.
31. Rehman, H.; Aziz, A.T.; Saggu, S.; VanWert, A.L.; Zidan, N.; Saggu, S. Additive Toxic Effect of Deltamethrin and Cadmium on Hepatic, Hematological, and Immunological Parameters in Mice. *Toxicol Ind Health* **2017**, *33*, 495–502, doi:10.1177/0748233716684710.
32. Saggu, S.; Rehman, H.; Aziz, A.T.; Alzeibr, F.M.A.; Oyouni, A.A.A.; Zidan, N.; Panneerselvam, C.; Trivedi, S. Cymbopogon Schoenanthus (Ethkher) Ameliorates Cadmium Induced Toxicity in Swiss Albino Mice. *Saudi J Biol Sci* **2019**, *26*, 1875–1881, doi:10.1016/j.sjbs.2017.01.002.
33. Sani, A.; Darma, A.I.; Abdullahi, I.L.; Musa, B.U.; Imam, F.A. Heavy Metals Mixture Affects the Blood and Antioxidant Defense System of Mice. *Journal of Hazardous Materials Advances* **2023**, *11*, 100340, doi:10.1016/j.hazadv.2023.100340.
34. Bist, P.; Singh, D.; Choudhary, S. Blood Metal Levels Linked with Hematological, Oxidative, and Hepatic-Renal Function Disruption in Swiss Albino Mice Exposed to Multi-Metal Mixture. *Comp Clin Path* **2023**, *32*, 477–490, doi:10.1007/s00580-023-03459-0.
35. Amedu, N.O.; Omotoso, G.O. Evaluating the Role of Vitexin on Hematologic and Oxidative Stress Markers in Lead-Induced Toxicity in Mice. *Toxicol Environ Health Sci* **2020**, *12*, 257–263, doi:10.1007/s13530-020-00039-5.
36. Ali, S.; Bashir, S.; Mumtaz, S.; Shakir, H.A.; Ara, C.; Ahmad, F.; Tahir, H.M.; Faheem, M.; Irfan, M.; Masih, A.; et al. Evaluation of Cadmium Chloride-Induced Toxicity in Chicks Via Hematological, Biochemical Parameters, and Cadmium Level in Tissues. *Biol Trace Elem Res* **2021**, *199*, 3457–3469, doi:10.1007/s12011-020-02453-9.
37. Matović, V.; Buha, A.; Đukić-Ćosić, D.; Bulat, Z. Insight into the Oxidative Stress Induced by Lead and/or Cadmium in Blood, Liver and Kidneys. *Food and Chemical Toxicology* **2015**, *78*, 130–140, doi:10.1016/j.fct.2015.02.011.
38. Yang, Z.; He, Y.; Wang, H.; Zhang, Q. Protective Effect of Melatonin against Chronic Cadmium-Induced Hepatotoxicity by Suppressing Oxidative Stress, Inflammation, and Apoptosis in Mice. *Ecotoxicol Environ Saf* **2021**, *228*, 112947, doi:10.1016/j.ecoenv.2021.112947.
39. Singhal, R.K.; Anderson, M.E.; Meister, A. Glutathione, a First Line of Defense against Cadmium Toxicity. *The FASEB Journal* **1987**, *1*, 220–223, doi:10.1096/fasebj.1.3.2887478.
40. Krupina, K.; Goginashvili, A.; Cleveland, D.W. Causes and Consequences of Micronuclei. *Curr Opin Cell Biol* **2021**, *70*, 91–99, doi:10.1016/j.ceb.2021.01.004.
41. Tapisso, J.T.; Marques, C.C.; Mathias, M. da L.; Ramalhinho, M. da G. Induction of Micronuclei and Sister Chromatid Exchange in Bone-Marrow Cells and Abnormalities in Sperm of Algerian Mice (Mus Spretus) Exposed to Cadmium, Lead and Zinc. *Mutation Research/Genetic Toxicology and Environmental Mutagenesis* **2009**, *678*, 59–64, doi:10.1016/j.mrgentox.2009.07.001.

 doi:10.20944/preprints202503.1874.v1

42. Mitkovska, V.I.; Dimitrov, H.A.; Chassovnikarova, T.G. Chronic Exposure to Lead and Cadmium Pollution Results in Genomic Instability in a Model Biomonitor Species (Apodemus Flavicollis Melchior, 1834). *Ecotoxicol Environ Saf* **2020**, *194*, 110413, doi:10.1016/j.ecoenv.2020.110413.
43. Çelik, A.; Mazmanci, B.; Çamlica, Y.; Aşkin, A.; Çömelekoğlu, Ü. Induction of Micronuclei by Lambda-Cyhalothrin in Wistar Rat Bone Marrow and Gut Epithelial Cells. *Mutagenesis* **2005**, *20*, 235–235, doi:10.1093/mutage/gei035.
44. Çelik, A.; Büyükakilli, B.; Çimen, B.; Taşdelen, B.; Öztürk, M.İ.; Eke, D. Assessment of Cadmium Genotoxicity in Peripheral Blood and Bone Marrow Tissues of Male Wistar Rats. *Toxicol Mech Methods* **2009**, *19*, 135–140, doi:10.1080/15376510802354979.
45. Fahmy, M.A..; Aly, F.A. In Vivo and in Vitro Studies on the Genotoxicity of Cadmium Chloride in Mice. *Journal of Applied Toxicology: An International Journal* **2000**, *20*, 231–238.
46. Belliardo, C.; Di Giorgio, C.; Chaspoul, F.; Gallice, P.; Bergé-Lefranc, D. Direct DNA Interaction and Genotoxic Impact of Three Metals: Cadmium, Nickel and Aluminum. *J Chem Thermodyn* **2018**, *125*, 271–277, doi:10.1016/j.jct.2018.05.028.
47. Beltcheva, M.; Ostoich, P.; Aleksieva, I.; Metcheva, R. Natural Zeolites as Detoxifiers and Modifiers of the Biological Effects of Lead and Cadmium in Small Rodents: A Review. *BioRisk* **2022**, *17*, 147–155, doi:10.3897/biorisk.17.77435.
48. EEA Heavy Metal Emissions in Europe.
49. Ramezani, M.; Enayati, M.; Ramezani, M.; Ghorbani, A. A Study of Different Strategical Views into Heavy Metal(Oid) Removal in the Environment. *Arabian Journal of Geosciences* **2021**, *14*, 2225, doi:10.1007/s12517-021-08572-4.
50. Raj, D.; Maiti, S.K. Sources, Bioaccumulation, Health Risks and Remediation of Potentially Toxic Metal(Loid)s (As, Cd, Cr, Pb and Hg): An Epitomised Review. *Environ Monit Assess* **2020**, *192*, 108, doi:10.1007/s10661-019-8060-5.
51. Commission Regulation (EU) No 744/2012 Annexes I and II to Directive 2002/32/EC of the European Parliament and the Council as Regards Maximum Levels for Arsenic, Fluorine, Lead, Mercury, Endosulfan, Dioxins, Ambrosia Spp., Diclazuril and Lasalocid A Sodium and Action Thresholds for Dioxins, Official J. of the EU, 1–8.
52. Commission Implementing Regulation (EU) No 651/2013 The Authorisation of Clinoptilolite of Sedimentary Origin as a Feed Additive for All Animal Species and Amending Regulation (EC) No 1810/2005, Official J. of the EU, 1–3.
53. Stefanova, I.; Djurova, E.; Gradev, G. Sorption of Zinc and Cadmium on Zeolite Rocks. *Journal of Radioanalytical and Nuclear Chemistry Letters* **1988**, *128*, 367–375, doi:10.1007/BF02205191.
54. Benoff, S.; Auborn, K.; Marmar, J.L.; Hurley, I.R. Link between Low-Dose Environmentally Relevant Cadmium Exposures and Asthenozoospermia in a Rat Model. *Fertil Steril* **2008**, *89*, e73–e79, doi:10.1016/j.fertnstert.2007.12.035.
55. Caflisch, C.R. Effect of Orally Administered Cadmium on in Situ PH, PCO_2, and Bicarbonate Concentration in Rat Testis and Epididymis. *J Toxicol Environ Health* **1994**, *42*, 323–330, doi:10.1080/15287399409531882.
56. Kim, J.E.; Nam, J.H.; Cho, J.Y.; Kim, K.S.; Hwang, D.Y. Annual Tendency of Research Papers Used ICR Mice as Experimental Animals in Biomedical Research Fields. *Lab Anim Res* **2017**, *33*, 171, doi:10.5625/lar.2017.33.2.171.
57. Friberg, L. Cadmium and the Kidney. *Environ Health Perspect* **1984**, *54*, 1–11, doi:10.1289/ehp.84541.
58. Şehirli, Ö.; Tozan, A.; Omurtag, G.Z.; Cetinel, S.; Contuk, G.; Gedik, N.; Şener, G. Protective Effect of Resveratrol against Naphthalene-Induced Oxidative Stress in Mice. *Ecotoxicol Environ Saf* **2008**, *71*, 301–308, doi:10.1016/j.ecoenv.2007.08.023.
59. Hayashi, M.; MacGregor, J.T.; Gatehouse, D.G.; Adler, I.-D.; Blakey, D.H.; Dertinger, S.D.; Krishna, G.; Morita, T.; Russo, A.; Sutou, S. In Vivo Rodent Erythrocyte Micronucleus Assay. II. Some Aspects of Protocol Design Including Repeated Treatments, Integration with Toxicity Testing, and Automated Scoring. *Environ Mol Mutagen* **2000**, *35*, 234–252, doi:10.1002/(SICI)1098-2280(2000)35:3<234::AID-EM10>3.0.CO;2-L.

60. Rudnick, R.L.; Gao, S. Composition of the Continental Crust. In *Treatise on Geochemistry*; Elsevier, 2014; pp. 1–51.
61. Tzvetanova, Y.; Tacheva, E.; Dimowa, L.; Tsvetanova, L.; Nikolov, A. Trace Elements in the Clinoptilolite Tuffs from Four Bulgarian Deposits, Eastern Rhodopes. *Rev. Bulg. Geol. Soc.* **2023**, *84*, 51–55.
62. Apreutesei, R.E.; Catrinescu, C.; Teodosiu, C. SURFACTANT-MODIFIED NATURAL ZEOLITES FOR ENVIRONMENTAL APPLICATIONS IN WATER PURIFICATION. *Environ Eng Manag J* **2008**, *7*, 149–161, doi:10.30638/eemj.2008.025.
63. Kraljević Pavelić, S.; Micek, V.; Filošević, A.; Gumbarević, D.; Žurga, P.; Bulog, A.; Orct, T.; Yamamoto, Y.; Preočanin, T.; Plavec, J.; et al. Novel, Oxygenated Clinoptilolite Material Efficiently Removes Aluminium from Aluminium Chloride-Intoxicated Rats in Vivo. *Microporous and Mesoporous Materials* **2017**, *249*, 146–156, doi:10.1016/j.micromeso.2017.04.062.
64. EFSA Panel on Additives and Products or Substances Used in Animal Feed (FEEDAP). Scientific Opinion on the Safety and Efficacy of Clinoptilolite of Sedimentary Origin for All Animal Species. *EFSA Journal* **2013**, *11*, 3039.
65. Beltcheva, M.; Tzvetanova, Y.; Todorova, T.; Tsvetanova, L.; Aleksieva, I.; Gerasimova, T.; Chassovnikarova, T. Does Natural Clinoptilolite Induce Toxicity in Small Mammals? *Acta Zool Bulg* **2024**, *76*, 289–297.
66. Ahmadi, M.; Kalinin, I.; Tomchuk, V. Removal of Heavy Metals Using Sorbents and Biochemical Indexes in Rats. *Ukrainian journal of veterinary sciences* **2023**, *14*, 9–22, doi:10.31548/veterinary4.2023.09.
67. Rodríguez-Iznaga, I.; Shelyapina, M.G.; Petranovskii, V. Ion Exchange in Natural Clinoptilolite: Aspects Related to Its Structure and Applications. *Minerals* **2022**, *12*, 1628, doi:10.3390/min12121628.
68. Bailey, S.E.; Olin, T.J.; Bricka, R.M.; Adrian, D.D. A Review of Potentially Low-Cost Sorbents for Heavy Metals. *Water Res* **1999**, *33*, 2469–2479, doi:10.1016/S0043-1354(98)00475-8.
69. Loizidou, M.; Townsend, R.P. Exchange of Cadmium into the Sodium and Ammonium Forms of the Natural Zeolites Clinoptilolite, Mordenite, and Ferrierite. *Journal of the Chemical Society, Dalton Transactions* **1987**, 1911, doi:10.1039/dt9870001911.
70. Sen Gupta, S.; Bhattacharyya, K.G. Adsorption of Metal Ions by Clays and Inorganic Solids. *RSC Adv.* **2014**, *4*, 28537–28586, doi:10.1039/C4RA03673E.
71. Demir, A.; Gunay, A.; Debik, E. Ammonium Removal from Aqueous Solution by Ion-Exchange Using Packed Bed Natural Zeolite. *Water SA* **2002**, *28*, doi:10.4314/wsa.v28i3.4903.
72. Wang, S.; Peng, Y. Natural Zeolites as Effective Adsorbents in Water and Wastewater Treatment. *Chemical Engineering Journal* **2010**, *156*, 11–24, doi:10.1016/j.cej.2009.10.029.
73. Rhodes, C.J. Zeolites: Physical Aspects and Environmental Applications. *Annual Reports Section "C" (Physical Chemistry)* **2007**, *103*, 287, doi:10.1039/b605702k.
74. Korkuna, O.; Leboda, R.; Skubiszewska-Zie¸ba, J.; Vrublevs'ka, T.; Gun'ko, V.M.; Ryczkowski, J. Structural and Physicochemical Properties of Natural Zeolites: Clinoptilolite and Mordenite. *Microporous and Mesoporous Materials* **2006**, *87*, 243–254, doi:10.1016/j.micromeso.2005.08.002.
75. Bist, R.B.; Subedi, S.; Chai, L.; Regmi, P.; Ritz, C.W.; Kim, W.K.; Yang, X. Effects of Perching on Poultry Welfare and Production: A Review. *Poultry* **2023**, *2*, 134–157, doi:10.3390/poultry2020013.
76. Pavelić, K., H.M. Medical Applications of Zeolites. In *Handbook of zeolite science and technology*; CRC press., 2003; pp. 1453–1491.
77. Kristo, A.S.; Tzanidaki, G.; Lygeros, A.; Sikalidis, A.K. Bile Sequestration Potential of an Edible Mineral (Clinoptilolite) under Simulated Digestion of a High-Fat Meal: An in Vitro Investigation. *Food Funct* **2015**, *6*, 3818–3827, doi:10.1039/C5FO00116A.
78. Haemmerle, M.M.; Fendrych, J.; Matiasek, E.; Tschegg, C. Adsorption and Release Characteristics of Purified and Non-Purified Clinoptilolite Tuffs towards Health-Relevant Heavy Metals. *Crystals (Basel)* **2021**, *11*, 1343, doi:10.3390/cryst11111343.
79. Klaassen, C.D.; Liu, J.; Choudhuri, S. METALLOTHIONEIN: An Intracellular Protein to Protect Against Cadmium Toxicity. *Annu Rev Pharmacol Toxicol* **1999**, *39*, 267–294, doi:10.1146/annurev.pharmtox.39.1.267.

 doi:10.20944/preprints202503.1874.v1

80. Elsenhans, B.; Strugala, G.; Schäfer, S. Small-Intestinal Absorption of Cadmium and the Significance of Mucosal Metallothionein. *Hum Exp Toxicol* **1997**, *16*, 429–434, doi:10.1177/096032719701600803.
81. Yang, H.; Shu, Y. Cadmium Transporters in the Kidney and Cadmium-Induced Nephrotoxicity. *Int J Mol Sci* **2015**, *16*, 1484–1494, doi:10.3390/ijms16011484.
82. Burmańczuk, A.; Markiewicz, W.; Burmańczuk, A.; Kowalski, C.; Roliński, Z.; Burmańczuk, N. Possibile Use of Natural Zeolites in Animal Production and Environment Protection. *J Elem* **2015**, doi:10.5601/jelem.2014.19.4.759.
83. Papaioannou, D.; Katsoulos, P.D.; Panousis, N.; Karatzias, H. The Role of Natural and Synthetic Zeolites as Feed Additives on the Prevention and/or the Treatment of Certain Farm Animal Diseases: A Review. *Microporous and Mesoporous Materials* **2005**, *84*, 161–170, doi:10.1016/j.micromeso.2005.05.030.
84. Kraljević Pavelić, S.; Saftić Martinović, L.; Simović Medica, J.; Žuvić, M.; Perdija, Ž.; Krpan, D.; Eisenwagen, S.; Orct, T.; Pavelić, K. Clinical Evaluation of a Defined Zeolite-Clinoptilolite Supplementation Effect on the Selected Blood Parameters of Patients. *Front Med (Lausanne)* **2022**, *9*, doi:10.3389/fmed.2022.851782.
85. Świergosz-Kowalewska, R. Cadmium Distribution and Toxicity in Tissues of Small Rodents. *Microsc Res Tech* **2001**, *55*, 208–222, doi:10.1002/jemt.1171.
86. Johnstone, C.P.; Lill, A.; Reina, R.D. Use of Erythrocyte Indicators of Health and Condition in Vertebrate Ecophysiology: A Review and Appraisal. *Biological Reviews* **2017**, *92*, 150–168, doi:10.1111/brv.12219.
87. Powolny, T.; Scheifler, R.; Raoul, F.; Coeurdassier, M.; Fritsch, C. Effects of Chronic Exposure to Toxic Metals on Haematological Parameters in Free-Ranging Small Mammals. *Environmental Pollution* **2023**, *317*, 120675, doi:10.1016/j.envpol.2022.120675.
88. Koçak, M.; Akçıl, E. The Effects of Chronic Cadmium Toxicity on the Hemostatic System. *Pathophysiol Haemost Thromb* **2006**, *35*, 411–416, doi:10.1159/000102047.
89. Nazima, B.; Manoharan, V.; Miltonprabu, S. Oxidative Stress Induced by Cadmium in the Plasma, Erythrocytes and Lymphocytes of Rats. *Hum Exp Toxicol* **2016**, *35*, 428–447, doi:10.1177/0960327115591376.
90. Hamilton, D.; Valberg, L. Relationship between Cadmium and Iron Absorption. *American Journal of Physiology-Legacy Content* **1974**, *227*, 1033–1037, doi:10.1152/ajplegacy.1974.227.5.1033.
91. Horiguchi, H.; Teranishi, H.; Niiya, K.; Aoshima, K.; Katoh, T.; Sakuragawa, N.; Kasuya, M. Hypoproduction of Erythropoietin Contributes to Anemia in Chronic Cadmium Intoxication: Clinical Study on Itai-Itai Disease in Japan. *Arch Toxicol* **1994**, *68*, 632–636, doi:10.1007/BF03208342.
92. Kolanjiappan, K.; Manoharan, S.; Kayalvizhi, M. Measurement of Erythrocyte Lipids, Lipid Peroxidation, Antioxidants and Osmotic Fragility in Cervical Cancer Patients. *Clinica Chimica Acta* **2002**, *326*, 143–149, doi:10.1016/S0009-8981(02)00300-5.
93. Minetti, M.; Pietraforte, D.; Straface, E.; Metere, A.; Matarrese, P.; Malorni, W. Red Blood Cells as a Model to Differentiate between Direct and Indirect Oxidation Pathways of Peroxynitrite. In; 2008; pp. 253–272.
94. Demir, H.; Kanter, M.; Coskun, O.; Uz, Y.H.; Koc, A.; Yildiz, A. Effect of Black Cumin (Nigella Sativa) on Heart Rate, Some Hematological Values, and Pancreatic β-Cell Damage in Cadmium-Treated Rats. *Biol Trace Elem Res* **2006**, *110*, 151–162, doi:10.1385/BTER:110:2:151.
95. El-Boshy, M.E.; Risha, E.F.; Abdelhamid, F.M.; Mubarak, M.S.; Hadda, T. Ben Protective Effects of Selenium against Cadmium Induced Hematological Disturbances, Immunosuppressive, Oxidative Stress and Hepatorenal Damage in Rats. *Journal of Trace Elements in Medicine and Biology* **2015**, *29*, 104–110, doi:10.1016/j.jtemb.2014.05.009.
96. Donmez, H.H.; Donmez, N.; Kısadere, I.; Undag, I. Protective Effect of Quercetin on Some Hematological Parameters in Rats Exposed to Cadmium. *Biotechnic & Histochemistry* **2019**, *94*, 381–386, doi:10.1080/10520295.2019.1574027.
97. Karuppasamy, R.; Subathra, S.; Puvaneswari, S. Haematological Responses to Exposure to Sublethal Concentration of Cadmium in Air-Breathing Fish, Channa Punctatus (Bloch). *J Environ Biol* **2005**, *26*, 123–128.
98. Morsy, A. S.; Manal, M.; Gad-El-Moula, H.; Dooa, O.; Hassan, M. S.; Nagwa, A.A. Blood picture, metabolites and minerals of rabbits as influenced by drinking saline water in Egypt, Global Journal of Advanced Research, 3(11) (2016) 1008-1017, doi: http://gjar.org/publishpaper/vol3issue11/d628r62.pdf

 doi:10.20944/preprints202503.1874.v1

99. Martin-Kleiner, I.; Flegar-Meštrić, Z.; Zadro, R.; Breljak, D.; Stanović Janda, S.; Stojković, R.; Marušić, M.; Radačić, M.; Boranić, M. The Effect of the Zeolite Clinoptilolite on Serum Chemistry and Hematopoiesis in Mice. *Food and Chemical Toxicology* **2001**, *39*, 717–727, doi:10.1016/S0278-6915(01)00004-7.
100. Mojzis, J.; Nistiar, F.; Kovac, G.; Mojzisova, G. Preventive Effect of Zeolite in VX Poisoning in Rats. *Veterinarni medicin* **1994**, *39*, 443–449.
101. Waisberg, M.; Joseph, P.; Hale, B.; Beyersmann, D. Molecular and Cellular Mechanisms of Cadmium Carcinogenesis. *Toxicology* **2003**, *192*, 95–117, doi:10.1016/S0300-483X(03)00305-6.
102. Pond, W. G.; Ming, D. W.; Mumpton, F. A. Zeolites in animal nutrition and health: a review. *Natural zeolites* **1995**, *93*, 449.
103. Liu, J.; Qu, W.; Kadiiska, M.B. Role of Oxidative Stress in Cadmium Toxicity and Carcinogenesis. *Toxicol Appl Pharmacol* **2009**, *238*, 209–214, doi:10.1016/j.taap.2009.01.029.
104. Hu, B.; Liu, S.; Luo, Y.; Pu, J.; Deng, X.; Zhou, W.; Dong, Y.; Ma, Y.; Wang, G.; Yang, F.; et al. Procyanidin B2 Alleviates Uterine Toxicity Induced by Cadmium Exposure in Rats: The Effect of Oxidative Stress, Inflammation, and Gut Microbiota. *Ecotoxicol Environ Saf* **2023**, *263*, 115290, doi:10.1016/j.ecoenv.2023.115290.
105. Valko, M.; Morris, H.; Cronin, M. Metals, Toxicity and Oxidative Stress. *Curr Med Chem* **2005**, *12*, 1161–1208, doi:10.2174/0929867053764635.
106. Ren, L.; Qi, K.; Zhang, L.; Bai, Z.; Ren, C.; Xu, X.; Zhang, Z.; Li, X. Glutathione Might Attenuate Cadmium-Induced Liver Oxidative Stress and Hepatic Stellate Cell Activation. *Biol Trace Elem Res* **2019**, *191*, 443–452, doi:10.1007/s12011-019-1641-x
107. Singh, C.; Singh, R.; Shekhar, A. Oxidative Stress in Cadmium Toxicity in Animals and Its Amelioration. In *Cadmium Toxicity Mitigation*; Springer Nature Switzerland: Cham, 2024; pp. 391–411.
108. Souza-Arroyo, V.; Fabián, J.J.; Bucio-Ortiz, L.; Miranda-Labra, R.U.; Gomez-Quiroz, L.E.; Gutiérrez-Ruiz, M.C. The Mechanism of the Cadmium-Induced Toxicity and Cellular Response in the Liver. *Toxicology* **2022**, *480*, 153339, doi:10.1016/j.tox.2022.153339.
109. Saribeyoglu, K.; Aytac, E.; Pekmezci, S.; Saygili, S.; Uzun, H.; Ozbay, G.; Aydin, S.; Seymen, H.O. Effects of Clinoptilolite Treatment on Oxidative Stress after Partial Hepatectomy in Rats. *Asian J Surg* **2011**, *34*, 153–157, doi:10.1016/j.asjsur.2011.11.007.
110. Abu-El-Zahab, H.S.H.; Hamza, R.Z.; Montaser, M.M.; El-Mahdi, M.M.; Al-Harthi, W.A. Antioxidant, Antiapoptotic, Antigenotoxic, and Hepatic Ameliorative Effects of L-Carnitine and Selenium on Cadmium-Induced Hepatotoxicity and Alterations in Liver Cell Structure in Male Mice. *Ecotoxicol Environ Saf* **2019**, *173*, 419–428, doi:10.1016/j.ecoenv.2019.02.041.
111. Huang, Y.; He, C.; Shen, C.; Guo, J.; Mubeen, S.; Yuan, J.; Yang, Z. Toxicity of Cadmium and Its Health Risks from Leafy Vegetable Consumption. *Food Funct* **2017**, *8*, 1373–1401, doi:10.1039/C6FO01580H.
112. Sun, Q.; Li, Y.; Shi, L.; Hussain, R.; Mehmood, K.; Tang, Z.; Zhang, H. Heavy Metals Induced Mitochondrial Dysfunction in Animals: Molecular Mechanism of Toxicity. *Toxicology* **2022**, *469*, 153136, doi:10.1016/j.tox.2022.153136.
113. Todorova, T.; Alexieva, I.; Ostoich, P.; Dimitrova, M.; Boyadzhiev, K.; Lyubomirova, L.; Beltcheva, M. Different Lead- and Cadmium-Induced Oxidative Stress Profiles in the Liver and Kidneys of Subchronically-Exposed Mice. *Acta Zool Bulg* **2023**, *75*, 343–349.
114. Mabbott, N.A.; Donaldson, D.S.; Ohno, H.; Williams, I.R.; Mahajan, A. Microfold (M) Cells: Important Immunosurveillance Posts in the Intestinal Epithelium. *Mucosal Immunol* **2013**, *6*, 666–677, doi:10.1038/mi.2013.30.
115. Panaiotov, S.; Tancheva, L.; Kalfin, R.; Petkova-Kirova, P. Zeolite and Neurodegenerative Diseases. *Molecules* **2024**, *29*, 2614, doi:10.3390/molecules29112614.
116. Qu, F.; Zheng, W. Cadmium Exposure: Mechanisms and Pathways of Toxicity and Implications for Human Health. *Toxics* **2024**, *12*, 388, doi:10.3390/toxics12060388.
117. Liu, N.; Du, J.; Ge, J.; Liu, S.-B. DNA Damage-Inducing Endogenous and Exogenous Factors and Research Progress. *Nucleosides Nucleotides Nucleic Acids* **2024**, 1–33, doi:10.1080/15257770.2024.2428436.

 doi:10.20944/preprints202503.1874.v1

118. Pereira, S.; Cavalie, I.; Camilleri, V.; Gilbin, R.; Adam-Guillermin, C. Comparative Genotoxicity of Aluminium and Cadmium in Embryonic Zebrafish Cells. *Mutation Research/Genetic Toxicology and Environmental Mutagenesis* **2013**, *750*, 19–26, doi:10.1016/j.mrgentox.2012.07.007.
119. Viau, M.; Sonzogni, L.; Ferlazzo, M.L.; Berthel, E.; Pereira, S.; Bodgi, L.; Granzotto, A.; Devic, C.; Fervers, B.; Charlet, L.; et al. DNA Double-Strand Breaks Induced in Human Cells by Twelve Metallic Species: Quantitative Inter-Comparisons and Influence of the ATM Protein. *Biomolecules* **2021**, *11*, 1462, doi:10.3390/biom11101462.